Stratigraphic and structural evolution of the middle Miocene synvolcanic Oregon-Idaho graben

Michael L. Cummings* *Department of Geology, Portland State University, P.O. Box 751, Portland, Oregon 97207, USA*
James G. Evans *U.S. Geological Survey, West 904 Riverside, Room 202, Spokane, Washington 99210, USA*
Mark L. Ferns *Oregon Department of Geology and Mineral Industries, 1831 First Street, Baker City, Oregon 97814, USA*
Kate R. Lees *Department of Earth Sciences, Open University, Milton Keynes, UK*

ABSTRACT

The Oregon-Idaho graben is a newly identified north-south–trending synvolcanic graben in southeastern Oregon and southwestern Idaho within the middle Miocene backarc rift system that extends 1100 km from southern Nevada to southeastern Washington. The graben formed along the western margin of the North American craton shortly after the largest volumes of tholeiitic flood basalt erupted (Columbia River Basalt Group, Steens-Pueblo Basalt, basalt of Malheur Gorge, basalt and latite unit of Ekren et al., 1981). Rhyolite flows and ash-flow tuffs (16.1–14.0 Ma) erupted from northeastern Oregon (Dooley Volcanics) to northern Nevada (McDermitt volcanic field) shortly after the flood basalt was emplaced. Subsidence of the Oregon-Idaho graben (15.5–15.3 Ma) coincides with eruption of rhyolite flows and caldera-related ash-flow tuffs from vents along the margins and within the graben. Mafic and silicic intragraben volcanism accompanied sedimentation from about 15.3 to 10.5 Ma. Sedimentary and volcanic rocks from extrabasinal sources, especially southwestern Idaho, were introduced periodically.

After initial subsidence, the evolution of the Oregon-Idaho graben is divided into three stages. Stage 1 (15.3–14.3 Ma) followed intragraben caldera collapse and was marked by deposition of fluvial and lacustrine sediment across the graben. Stage 2 (14.3–12.6 Ma) movement on intragraben fault zones divided the graben into distinct subbasins and marked the onset of calc-alkalic volcanism. Fine-grained tuffaceous sediment derived from glassy rhyolite and pyroclastic deposits and basalt tuff cones interbedded with rhyolite ash and lapilli-fall deposits and locally erupted basalt hydrovolcanic deposits predominated during synvolcanic subsidence. Synsedimentary hot-spring alteration and precious-metals mineralization of graben fill were controlled by the same intragraben fault zones that served as magmatic conduits. During stage 3 (12.6–10.5 Ma) the subbasins were filled, and graben-wide fluviatile and lacustrine sedimentation resumed. At about the same time, renewed rhyolitic volcanism occurred on both flanks, and tholeiitic volcanism resumed within the Oregon-Idaho graben. Subsidence in the Oregon-Idaho graben ceased as west-northwest–striking faults related to the formation of the western Snake River plain became active.

Keywords: extension tectonics, fault zone, geologic history, graben, Malheur County Oregon, Miocene, volcaniclastic rocks.

INTRODUCTION

The Oregon-Idaho graben was identified as a result of new geologic mapping in southeastern Oregon by the authors from 1987 to 1993 (Ferns et al., 1993a, 1993b; Cummings et al., 1994). In this paper, we review evidence for the existence of the graben and its associated volcanism, sedimentation, and precious-metals mineralization in the middle and late Miocene and relate the structure to regional extension responsible for the northern Nevada rift (Zoback et al., 1994) and extrusion of the Columbia River Basalt Group (Hooper and Conrey, 1989).

Continental flood basalt began to erupt during the Miocene (ca. 17.5 Ma) from vents near the concealed western margin of the North American craton as reflected in the strontium and neodymium isotopic ratios of igneous rocks (Armstrong et al., 1977; Carlson and Hart, 1987; Leeman et al., 1992). This volcanism has been ascribed to several processes including backarc spreading (Eaton, 1984; Hart et al., 1984; Zoback et al., 1994), meteorite impact (Alt et al., 1988), clockwise rotation of the Cascade-Klamath-Sierran blocks (Magill and Cox, 1981; Rytuba and Vander Meulen, 1991), and the migration of North America over the Yellowstone hot spot (Brandon and Goles, 1988; Draper, 1991; Pierce and Morgan, 1992; Geist and Richards, 1993, Zoback et al., 1994).

During the waning phase of this widespread outpouring of tholeiitic basalt, the Oregon-Idaho graben evolved as a 50–60-km-wide, 100-km-long, north-trending, generally topographically subdued synvolcanic graben adjacent to the inferred western margin of the North American craton approximately between lat 43°20′N and 44°05′N (Fig. 1). The relatively large-volume middle Miocene rhyolite flows and pyroclastic rocks that erupted after the flood basalt are partly contemporaneous with the development of the graben. The Oregon-Idaho graben lies between the northern Nevada rift (Zoback and Thompson, 1978; Zoback et al., 1994) and the dike swarms for the Imnaha and Grande Ronde Formations of the Columbia River Basalt Group (Fig. 1).

Present topographic expression of the Oregon-Idaho graben is generally subdued. On the northeast, the graben is truncated by late Miocene to Quaternary faults that define the southwestern margin of the western Snake River plain and by more subtle faults identified by abrupt stratigraphic changes from middle to upper Miocene sediment, pyroclastic rock, and relatively small-volume lava flows (Fig. 2). Part of the eastern margin is buried by the 11 Ma Jump Creek Rhyolite. The southeastern margin is a series of

*E-mail: cummingsm@pdx.edu.

GSA Bulletin; May 2000; v. 112; no. 5; p. 668–682; 8 figures; 2 tables.

north-striking faults located immediately east of the Oregon-Idaho state line. The north- to north-northeast–trending western margin of the graben is defined by middle Miocene fault zones that juxtapose resistant flood basalt and other well-lithified volcanic rocks with the generally poorly lithified sedimentary rocks of the graben. The fault zones have been sites for intrusion of the Littlefield Rhyolite and Hunter Creek Basalt (icelandite) and indicate that some of the graben subsidence was contemporaneous with silicic to intermediate volcanism (Evans, 1990a; Brooks and O'Brien, 1992; Evans and Binger, 1998). Quaternary erosion has excavated the more easily eroded graben-fill sediments and produced appreciable topographic relief along parts of the western graben margin. On the southern side, a Pliocene to Holocene basalt field buries the graben. Middle Miocene graben-fill sedimentary rocks onlap flood basalts at the northern end of the graben.

BASEMENT OF THE OREGON-IDAHO GRABEN

Rare inclusions in volcanic rocks of the Oregon-Idaho graben and adjacent to the graben indicate the character of the pre-Tertiary basement. Xenoliths of chert and argillite containing recrystallized radiolaria tests in icelandite and rhyolite pyroclastic flows vented at Westfall Butte (Evans and Binger, 1997; Figs. 1 and 2), 20 km west of the graben, are indicative of the Blue Mountains accreted terranes, which project southward under the Tertiary rocks. These xenoliths are located approximately 30 km southwest of the nearest outcrop of radiolarian chert in the accreted terranes. Granitic gneiss inclusions in ferro-latites on the southwest flank of the graben near Crowley (Ferns and Williams, 1993; Fig. 1) and in basalt flows in the center of the graben (Cummings, 1991a) indicate underlying, possibly cratonic, metamorphic basement. These xenoliths may support the suggestion of Leeman et al. (1992), based on neodymium and strontium isotopic ratios in Miocene volcanic rocks, that the cratonic lithosphere extends farther to the west than the $^{87}Sr/^{86}Sr = 0.706$ line of Armstrong et al. (1977), which is poorly delineated in this part of Oregon.

The distribution of lower Tertiary rocks in southeastern Oregon and southwestern Idaho suggests the nature of Tertiary rocks beneath the flood basalt and graben. These lower Tertiary rocks include upper Oligocene–lower Miocene silicic pyroclastic and calc-alkalic lavas exposed in southwestern Idaho (Ekren et al., 1981), at the base of Steens Mountain (Blank and Gettings, 1974; Minor et al., 1987a; Vander Meulen et al., 1988; Walker and MacLeod, 1991), Hart Mountain (Mathis, 1993), Warner Range (Duffield and McKee, 1986; Wells, 1979) and near Unity Reservoir (Brooks et al., 1979) (see Fig. 1). Inclusions of rhyolitic welded tuff entrained in basaltic welded tuff are present in middle Miocene basalt flows exposed along the Malheur River Gorge (Evans, 1990a, 1990b).

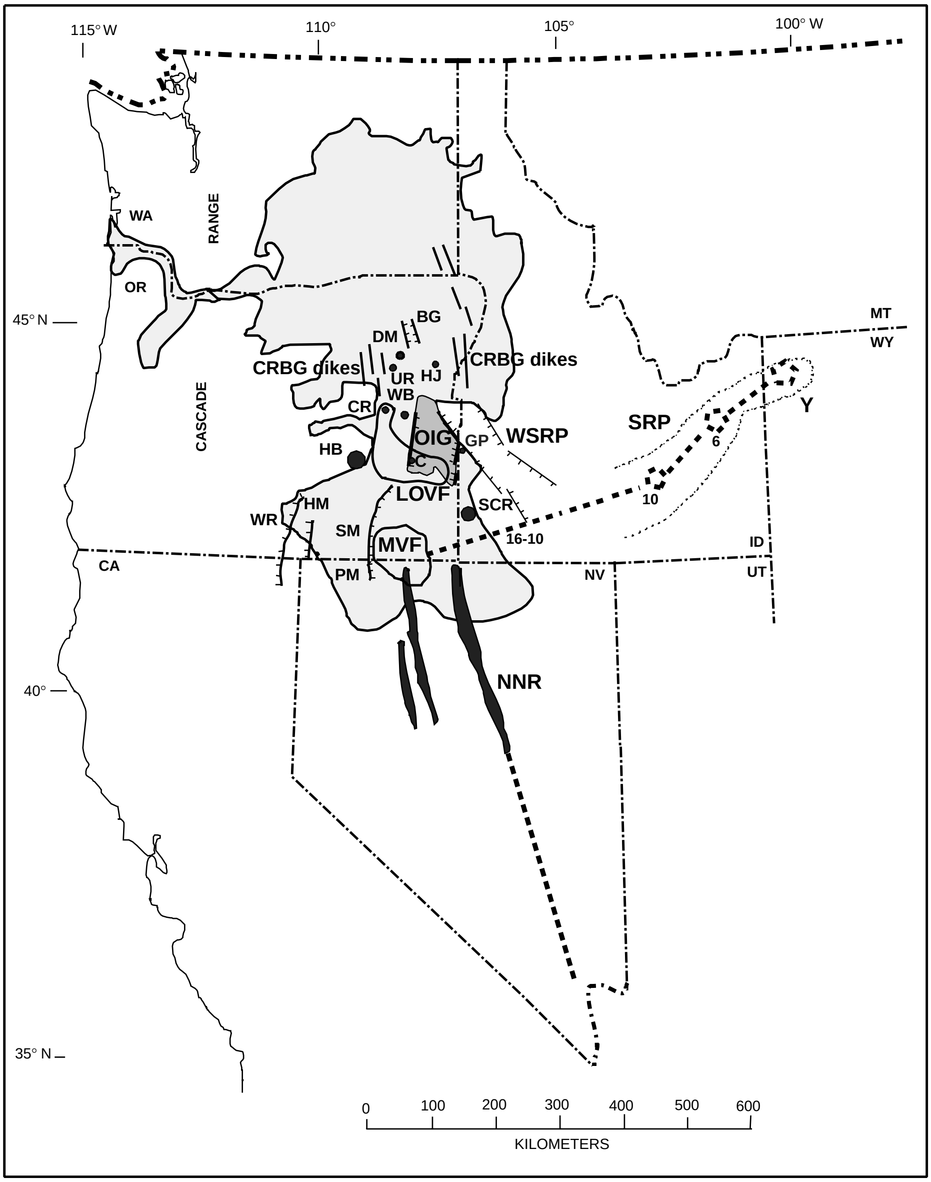

Figure 1. Regional map showing the Oregon-Idaho graben (OIG) in context of the dike swarms of the Columbia River Basalt Group (CRBG dikes), the northern Nevada rift (NNR), and the western Snake River plain (WSRP). Regional features in the vicinity of the Oregon-Idaho graben depicted by additional symbols as follows: BG—Baker graben; C—Crowley; CR—Castle Rock; DM—Dooley Mountain; GP—Graveyard Point, HB—Harney basin; HJ—Huntington Junction; HM—Hart Mountain; LOVF—Lake Owyhee volcanic field; MVF—McDermitt volcanic field; PM—Pueblo Mountains; SM—Steens Mountain; SCR—Silver City Range; SRP—Snake River plain; WB—Westfall Butte; WR—Warner Range; UR—Unity Reservoir; Y—Yellowstone Plateau. WA—Washington; OR—Oregon; ID—Idaho; MT—Montana; WY—Wyoming; UT—Utah; NV—Nevada; CA—California. Numbers displayed along the Snake River plain (SRP) show the age progression of rhyolitic volcanism.

FLOOD BASALT VOLCANISM AND GRABEN DEVELOPMENT

Development of the Oregon-Idaho graben followed eruptions of large volumes of tholeiitic basalts on the Oregon and Columbia Plateaus.

Thick sections of time-correlative tholeiitic basalt accumulated in southwestern Idaho (>0.6–1 km; Pansze, 1975; Ekren et al., 1982), in the Pueblo Mountains (1 km) and Steens Mountain (>1 km) (Hart et al., 1989), along the Malheur River (>0.6 km; Evans, 1990a, 1990b), at Jones Butte (1 km; Evans, 1996), and at Graveyard Point (>130 m; Ferns, 1989; Ekren et al., 1982) (see Fig. 1). Flows of the Columbia River Basalt Group erupted from dike swarms located north of the Oregon-Idaho graben and covered over 163 700 km^2 of Oregon, Washington, and Idaho (Tolan et al., 1989). Other flood basalts covered another 65 000 km^2 in southeastern Oregon, southwestern Idaho, and northern Nevada (Carlson and Hart, 1988).

Near the western margin of the graben, the middle Miocene basalt of Malheur Gorge (Fig. 3A) includes interbedded tholeiitic lava flows and mafic pyroclastic deposits (Evans, 1990a, 1990b). Lowermost exposures consist of coarse, plagioclase-phyric basalt that is petrographically, geochemically, and geochronologically equivalent to the lowest coarse plagioclase-phyric basalt of the Steens Basalt in the Steens–Pueblo Mountains area (Fig. 1). The overlying flows are sparsely plagioclase phyric and are petrographically and geochemically equivalent to the Imnaha Basalt of the Columbia River Basalt Group (Lees, 1994; Binger, 1997). A mean of two $^{40}Ar/^{39}Ar$ age determinations yields a date of 16.5 Ma for the basalt of Malheur Gorge (Table 1). Baksi (1989) reports ages of 17.3 to 17.0 Ma for the Imnaha Basalt, and Hart et al. (1989) reported an age of 17.03 ± 0.28 Ma for coarsely plagioclase-phyric basalt from the Pueblo Basalt (Fig. 1). Some of the plagioclase-phyric basalts were erupted from a shield volcano (>10 km^2) located in the Jones Butte area (Evans, 1990a, 1996; Fig. 4A).

In the Malheur Gorge section, the aphyric basaltic andesite to icelandite (as defined by Carmichael, 1964) of the top part of the basalt of Malheur Gorge and the overlying Hunter Creek Basalt (Table 2; Kittleman et al., 1965, 1967) interfinger with rhyolitic ash-flow tuffs and large-volume rhyolite lava flows. The aphyric upper lavas of the basalt of Malheur Gorge are petrographically and geochemically equivalent to the Grande Ronde Basalt of the Columbia River Basalt Group (Lees, 1994; Binger, 1997).

A 1-km-thick section of tholeiitic lavas (Fig. 3A) present on the east margin of the Oregon-Idaho graben is interbedded with latite flows and tuffs (Ekren et al., 1982). Upper flows of the basalt of Bishop's Ranch, exposed near Graveyard Point (Fig. 4A and Table 2) include tholeiitic basalt, icelandite, and ferrodacite (Ferns, 1989) characterized by higher alumina contents than either the aphyric basalt of Malheur Gorge, Hunter Creek Basalt (icelandite), or Grande Ronde basalt flows. Pansze (1975) reported a K-Ar age of 17 Ma for one of these flows (Table 1). Tholeiitic lavas similar in composition to the Bishop's Ranch flows are exposed in topographically low positions on the south flank of Mahogany Mountain (MacLeod, 1990a, 1990b; Fig. 4A).

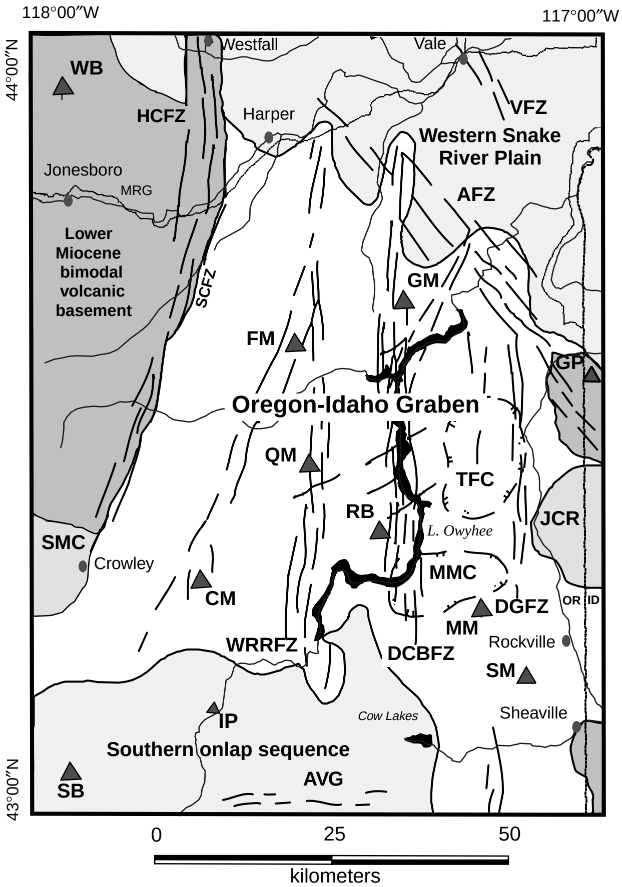

Figure 2. General geologic map of the Oregon-Idaho graben. AFZ—Adrian fault zone; AVG—Antelope Valley graben; CM—Cedar Mountain; DCBFZ—Dry Creek Buttes fault zone; DGFZ—Devils Gate fault zone; FM—Freezeout Mountain; GM—Grassy Mountain; GP—Graveyard Point; HCFZ—Hog Creek fault; IP—Iron Point; JCR—Jump Creek Rhyolite; MM—Mahogany Mountain; MMC—Mahogany Mountain caldera; MRG—Malheur River gorge; QM—Quartz Mountain; RB—Red Butte; SB—Saddle Butte; SCFZ—Squaw Creek fault zone; SMC—Star Mountain caldera; TFC—Three Fingers caldera; VFZ—Vale fault zone; WB—Westfall Butte; WRRFZ—Wall Rock Ridge fault zone. OR—Oregon; ID—Idaho.

EARLY RHYOLITE VOLCANISM

Middle Miocene rhyolite volcanism in eastern Oregon seldom receives attention relative to the earlier mafic tholeiitic volcanics. Between 16.5 and 15.3 Ma (Table 1), significant volumes of rhyolite erupted from a north-south belt of vents from Dooley Mountain and Unity Reservoir area on the north (Evans, 1992), through the Lake Owyhee volcanic field in the Oregon-Idaho graben (Rytuba et al., 1991), to the McDermitt volcanic field, which exceeds a volume >10 000 km^3, and which is located near the terminus of the northern Nevada rift (see Fig. 1; Wallace et al., 1980; Rytuba and McKee, 1984).

Along the west side of the Oregon-Idaho graben, ash-flow tuffs and rhyolite lava flows from both intragraben and extragraben vents interfinger with tholeiitic basalts. The Dinner Creek Welded Tuff (Kittleman et al., 1965; Haddock, 1967), dated at 15.3 Ma (see Table 1), is a weakly peralkaline rhyolite that erupted from a vent north or northwest of the graben. Calderas associated with the Dinner Creek Welded Tuff have been suggested in the Castle Rock area (Rytuba et al., 1991; Fig. 1) and in an area north of Westfall Butte (Evans and Binger, 1997; Figs. 1 and 2). The Dinner Creek Welded Tuff is a prominent marker between the upper flows of the basalt of Malheur Gorge and the Hunter Creek Basalt west of the Oregon-Idaho graben. The Dinner Creek thins from >120 m in the north near its source to as little as 3 m to the southeast; in places, it is absent. The mean age for the Hunter Creek Basalt ($^{40}Ar/^{39}Ar$; Table 1) is 15.4 ± 0.67 Ma, which is within the error of the K-Ar age determinations for the Dinner Creek Welded Tuff. Lenses of glass with the composition of the Hunter Creek Basalt within the Dinner Creek Welded Tuff suggest, however, that the magmas were in contact and that the time interval between eruptions was in all likelihood brief (Evans, 1990b; Evans and Binger, 1998).

Eruption of rhyolite flows along the western margin occurred during initial subsidence of the Oregon-Idaho graben and shortly before and after eruption of the Hunter Creek Basalt. The rhyolite of Cottonwood Mountain (J.G. Evans, 1994, unpub. mapping, Swede Flat 7.5′ quadrangle; Fig. 4A) is a >200-m-thick plagioclase-phyric rhyolite flow that is overlain by Hunter Creek Basalt that, in turn, is overlain by the plagioclase-phyric Littlefield Rhyolite (Table 2; Kittleman et al., 1965; Evans and Binger, 1998).

The rhyolite of Cottonwood Mountain erupted at around 15.2 Ma (Table 1) after subsidence of the graben as shown by feeder dikes cutting tuffaceous sedimentary rocks (J.G. Evans, 1994, unpub. mapping, Hope Butte 7.5′ quadrangle), and is extensive north of lat 44°N (area not shown in Fig. 4A). The Littlefield Rhyolite erupted from several vents (Benson and Kittleman, 1968), the largest of which may be in upper Simmons Gulch (Fig. 4A), marked by a circular aeromagnetic high and an extremely thick section of rhyolite (>365 m; Evans and Keith, 1996). Linear vents, such as the one identified near the western edge of the Littlefield exposures, trend north-south parallel to synvolcanic faults (Evans, 1990b). Synvolcanic, down-to-the-east movement along the Hog Creek fault zone (Fig. 4A) is indicated by abrupt thinning of the Littlefield Rhyolite from 300 m east of the fault to 50 m west of the fault (Fig. 4B). Farther south, the Littlefield Rhyolite flows ponded against highlands to the west and may have flowed southward along a fault-bounded trough and extended westward through topographic lows in the bounding escarpment. Conglomeratic fan deposits containing angular clasts of basalt of Malheur Gorge underlie the Littlefield Rhyolite in this portion of the western margin of the Oregon-Idaho graben (Figs. 4A and 4B). The Hog Creek fault zone and its southern extension, the northeast-trending Squaw

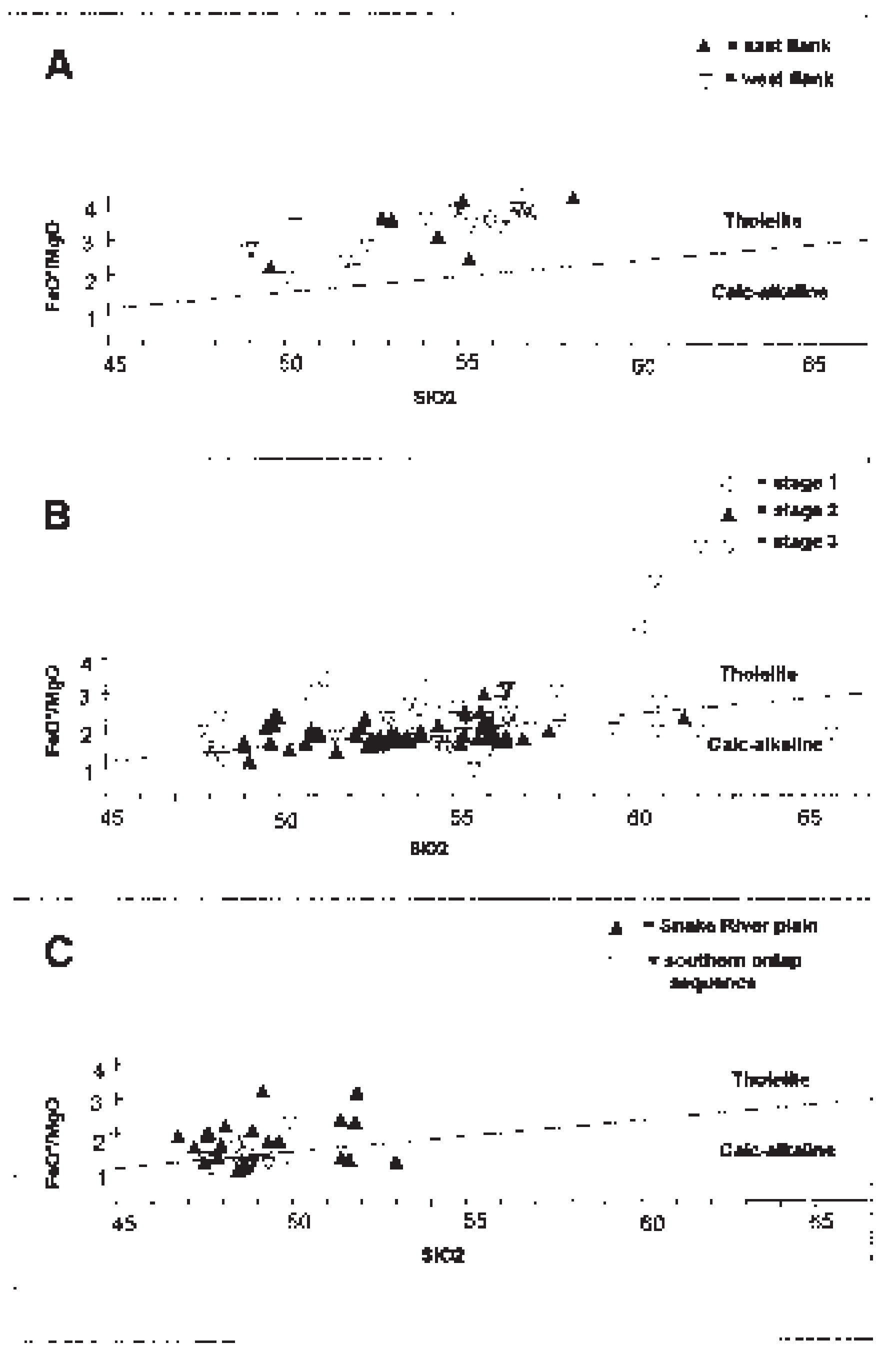

Figure 3. Discriminant diagram (after Miyashiro, 1975) for volcanic rocks in study area. Calc-alkaline rocks first appeared during stage 2 of graben development.

Creek fault zone, marked the western margin of the Oregon-Idaho graben during much of the graben subsidence.

East and southeast of the Oregon-Idaho graben, middle Miocene rhyolite erupted from vents in the Silver City Range between 15.2 and 16.1 Ma (Fig. 1 and Table 1). Younger Leslie Gulch and Spring Creek ash flows erupted from vents within the Oregon-Idaho graben at 15.5–15.4 Ma during the collapse of the Mahogany Mountain and Three Fingers calderas (Rytuba et al., 1991; Fig. 4A). The tuff of Leslie Gulch, a zoned peralkaline comendite to high-silica rhyolite (Vander Meulen, 1989) and the tuff of Spring Creek, a zoned metaluminous rhyolite, make up part of the Lake Owyhee volcanic field of Rytuba et al. (1991). Consistent north-south strikes of linear rhyolite dikes at the core of the Mahogany Mountain caldera (Vander Meulen, 1989) suggest east-west extension as these calderas formed. Slightly younger quartz-sanidine- and sanidine-phyric, high-silica rhyolite domes and shallow intrusions (15.2 to 14.9 Ma; Table 1) mark the inferred eastern margins of both calderas (Rytuba et al., 1989). A probable middle Miocene caldera, partly exposed at Iron Point where the Owyhee River cuts through concealing younger deposits (Figs. 2 and 4A), is also part of the Lake Owyhee volcanic field.

Faulted remnants of outflow sheets from intragraben calderas crop out atop basalt of Bishop's Ranch flows on the east flank of the Oregon-Idaho graben (Ferns, 1989; Fig. 4B). Outflow remnants appear confined to north-northeast–trending lows in an area east of the thickest exposures of tholeiite and may indicate early, down-to-the-west faulting along the east margin of the Oregon-Idaho graben prior to emplacement of the ash flows.

Constructional highs were relatively small, mainly silicic, pyroclastic vents on the flanks of the Mahogany Mountain and Three Fingers calderas following the eruption of the major rhyolite lava flows and ash-flow sheets between 15.4 and 15.0 Ma. The tuff of Birch Creek, a biotite- and hornblende-phyric rhyolite ash flow, was erupted with contemporaneous rhyolite domes just west of the Mahogany Mountain caldera (Plumley, 1986; Fig. 4A). The Honeycomb Hills is a small silicic eruptive center made up of coalescing silicic pyroclastic vents built up prior to collapse of the Three Fingers caldera (Fig. 4A).

Sparse structural data from small horsts west of the Mahogany Mountain caldera indicate a period of low-angle normal faulting with block rotation followed by erosion (M.L. Cummings, 1992, unpub. mapping, Big Mud Flat 7.5′ quadrangle). Low-angle faults (< 45°) are also exposed low in the section along Succor Creek, northeast of the Three Fingers caldera (Ferns, 1988; Lawrence, 1988).

TABLE1. RADIOMETRIC AGE DETERMINATIONS FOR ROCKS ASSOCIATED WITH THE OREGON-IDAHO GRABEN

Rock unit	Method	Age (Ma)	Reference
Pre-graben			
McDermitt volcanic field	K/Ar	15.0 – 16.1	Rytuba and McKee (1984)
Pueblo Basalt	K/Ar	15.20 – 17.03	Hart et al. (1989)
Basalt of Bishop's Ranch	K/Ar	17	Pansze (1975)
Rhyolite of Silver City Range	K/Ar	16.1 ± 0.3	Ekren et al. (1982)
Dinner Creek Welded Tuff	K/Ar	14.7 ± 0.4	Fiebelkorn et al. (1983)
		15.3 ± 0.4	
Basalt of Malheur Gorge	^{40}Ar/^{39}Ar	16.5 ± 0.62	This study
Stage 3			
Basalt of Stockade Mountain	K/Ar	11.3 ± 0.5	Fiebelkorn et al. (1983)
Jump Creek Rhyolite	K/Ar	11.1 ± 0.2	Armstrong et al. (1980)
Rhyolite of Pole Creek Top (Jump Creek Rhyolite)	K/Ar	10.6 ± 0.3	Rytuba et al. (1991)
Andesite of Vines Hill (FM)	^{40}Ar/^{39}Ar	10.2 ± 0.94	This study
Andesite of Freezeout Mountain (FM)	^{40}Ar/^{39}Ar	11.5 ± 0.99	Lees (1994)
Basalt of Grassy Mountain	K/Ar	10.18 ± 1.72	Hart (1982)
Andesite of Negro Rock	^{40}Ar/^{39}Ar	12.4 ± 0.8	Lees (1994)
	^{40}Ar/^{39}Ar	12.81±0.6	This study
Tuff of Kern Basin	K/Ar	12.6 ± 0.6	Ferns and Cummings (1992)
Mahogany gold prospect	K/Ar (adularia)	12.6 ± 0.6	Rytuba et al. (1991)
Stage 2			
Dam rhyolite	K/Ar	22.8 ± 2.6	Brown and Petros (1985)
	K/Ar	13.5 ± 3.4	Ferns and Cummings (1992)
Owyhee Basalt (upper)	K/Ar	13.4 ± 0.3	Watkins and Baksi (1974)
	K/Ar	13.3 ± 0.3	
	K/Ar	13.1 ± 0.3	
	K/Ar	16.4 ± 0.3	
	K/Ar	13.6 ± 0.3	
	^{40}Ar/^{39}Ar	14.3 ± 0.3	Bottomly and York (1976)
	K/Ar	15.3 ± 0.6	Brown and Petros (1985)
	K/Ar	22.8 ± 2.6	
Basalt of Succor Creek	^{40}Ar/^{39}Ar	13.08 ± 0.56	Lees (1994)
Blackjack Basalt	K/Ar	12.8 ± 0.4	Ferns and Cummings (1992)
	K/Ar	10.3 ± 1.1	
Tuff of Swisher Mountain	K/Ar	13.5 ± 0.2	Armstrong et al. (1980)
Bannock Ridge rhyolite	K/Ar	12.8 ± 0.3	Vander Meulen (1989)
Stage 1			
Rhyolite domes/plugs/dikes	K/Ar	15.2 ± 0.5 to 14.9 ± 0.4	Rytuba et al. (1989, 1991)
Initial subsidence			
Hunter Creek Basalt	^{40}Ar/^{39}Ar	15.89 ± 0.26	Lees (1994)
	^{40}Ar/^{39}Ar	15.4 ± 0.67	This study
Rhyolite of Cottonwood Mountain	^{40}Ar/^{39}Ar	15.24 ± 0.31	Lees (1994)
Tuff of Leslie Gulch	K/Ar	15.5 ± 0.5	Vander Meulen et al. (1987)
Tuff of Spring Creek	K/Ar	15.4	Rytuba and Vander Meulen (1991)
Post-graben			Hart and Mertzman (1983)
Basalts of Antelope Valley graben	K/Ar	1.86 ± 0.19 to 0.03 max.	Hart and Mertzman (1983)
WSRP tholeiites	K/Ar	7.8	Fiebelkorn et al. (1983)
Double Mountain dome	K/Ar	8.07 ± 0.21	MacLeod et al. (1976)
Devine Canyon Tuff	K/Ar	9.2	Walker (1990)
	^{40}Ar/^{39}Ar	9.68 ± 0.03	Streck et al. (1999)

PRINCIPAL STAGES OF GRABEN EVOLUTION

Structural evolution of the Oregon-Idaho graben was accompanied by intragraben volcanism and sedimentation and by introduction of sedimentary and volcanic deposits from extrabasinal sources, largely from southwestern Idaho. Although complex in detail, after initial subsidence of the Oregon-Idaho graben near the time of caldera formation, the graben passed through three stages. Stage 1 (15.3–14.3 Ma), following intragraben caldera collapse, was marked by deposition of fluvial and lacustrine sediments possibly across the width of the graben. During stage 2 (14.3–12.6 Ma), associated with synvolcanic collapse along intragraben faults, the Oregon-Idaho graben was subdivided into subbasins. Stage 2 was accompanied by calc-alkalic magmatism within the Oregon-Idaho graben. Stage 3 (12.6–10.5 Ma) was a period of intragraben sedimentary and volcanic aggradation that exceeded subsidence. Stage 2 subbasins were filled with sedimentary and volcanic material and lacustrine and fluvial sediments were again deposited across the width of the Oregon-Idaho graben. The Oregon-Idaho graben ceased as a synvolcanic graben at about 10.5 Ma as extension migrated to the western Snake River plain and west-northwest–trending structures related to the formation of the western Snake River plain graben truncated the northeastern part of the Oregon-Idaho graben.

Stage 1 (15.3–14.3 Ma)

First-stage deposits (Fig. 5, A and B) include arkosic channel sandstone and tuffaceous flood-

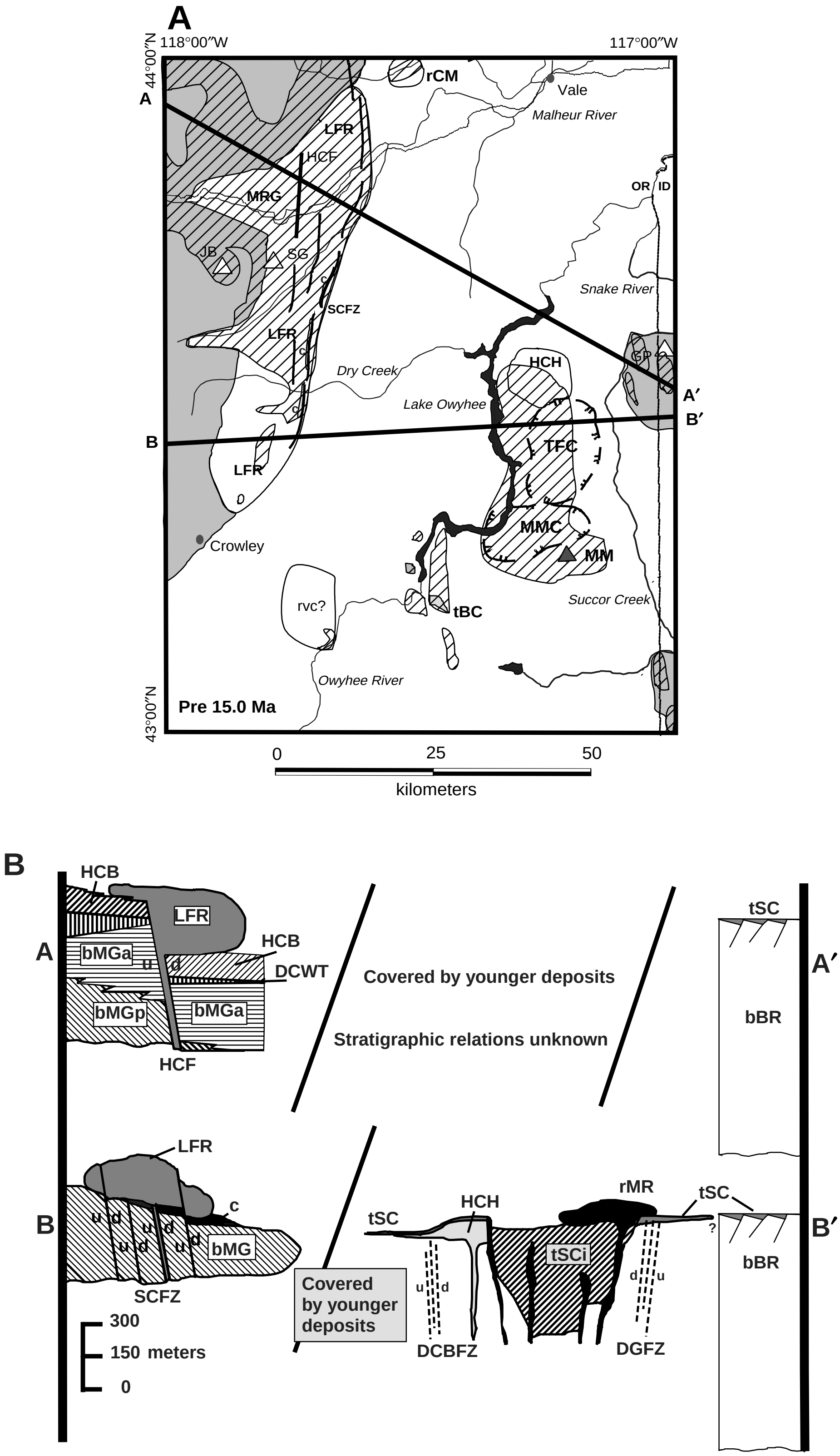

Figure 4. Pre–stage 1. (A) Inferred distribution of geologic features developed pre–stage 1 (>15.3 Ma) and modern exposure of rocks of this age (ruled pattern) in Oregon-Idaho graben. (B) Schematic diagram showing stratigraphic relations along section A–A′ and B–B′. Symbols: bBR—basalt of Bishop's Ranch; bMG—basalt of Malheur Gorge (bMGa—aphyric; bMGp—phyric); c—conglomerate; DCWT—Dinner Creek Welded Tuff; GP—Graveyard Point; HCB—Hunter Creek Basalt; HCF—Hog Creek fault; HCH—Honeycomb Hills; JB—Jones Butte; LFR—Little Field Rhyolite; MM—Mahogany Mountain; MMC—Mahogany Mountain caldera; rCM—rhyolite of Cottonwood Mountain; rMR—rhyolite of McIntyre Ridge; rvc?—rhyolite volcanic center or caldera; SCFZ—Squaw Creek fault zone; SG—Simmons Gulch; tBC—tuff of Birch Creek; TFC—Three Fingers caldera; tSC—tuff of Spring Creek; tSCi—tuff of Spring Creek intracaldera facies. ID—Idaho; OR—Oregon.

plain sandstone, siltstone, and mudstone. This sediment onlapped constructional highs formed by coalescing silicic pyroclastic deposits and post-caldera (Mahogany Mountain and Three Fingers calderas) domes. Basal strata include small-volume basalt hydrovolcanic deposits erupted along intragraben fault zones and brown to gray-brown tuffaceous silt and mudstone that lie unconformably on an eroded surface of caldera-related rhyolites. Subtle angular unconformities (5°–8°) within the mudstone and siltstone grade laterally to conformable contacts away from intragraben fault zones, suggesting syndepositional deformation along the fault zones. The overlying beds consist of muscovite-bearing, lithic-to-tuffaceous arkosic channel sands eroded from Tertiary, granite-cored highlands to the east and contemporary sandstone and siltstone floodplain deposits that contain mostly rhyolitic detritus derived from nearby intragraben rhyolites. Cross-bedding, channel- and fossil-tree-branch current indicators show southeast to northwest transport roughly sub-parallel to the graben axis (Fig. 5A). Conglomeratic fan deposits continued to be deposited locally along the west margin of the graben (Fig. 5, A and B).

Stage 2 (14.3–12.6 Ma)

Syntectonic calc-alkalic volcanism commenced in stage 2 (Fig. 3B) and is marked by increased basalt hydrovolcanism localized along intragraben fault zones and the abrupt disappearance of muscovite-bearing arkosic sediments. The Oregon-

TABLE 2. WHOLE-ROCK GEOCHEMISTRY OF REPRESENTATIVE SAMPLES OF SELECTED ROCK UNITS ASSOCIATED WITH THE OREGON-IDAHO GRABEN

Oxides (wt%)	Sample number*																			
	USBM 35	USBM 75	AXB 715	AXB 709	87-BO 35	87-BO 29	87-BO 72	87-BO 199	87-BO 104	AXB 301	AXB 308	AXB 312	AXB 324	OW 1044	OW 1481	AXB 511	AWB 111	AWB 100	AWB 101	OW 1083
SiO_2	50.02	48.58	54.1	72.1	53.3	65.0	73.8	53.9	52.8	67.5	48.8	52.7	51.8	70.2	74.0	55.8	72.1	69.0	47.3	53.3
Al_2O_3	14.53	15.53	13.2	13.2	15.6	13.2	12.0	16.5	15.6	15.0	15.1	16.7	16.3	14.3	13.1	16.4	12.7	14.4	15.2	16.5
TiO_2	2.02	1.87	2.35	0.07	1.42	1.19	0.30	1.09	1.62	0.48	2.38	1.24	1.36	0.47	0.19	1.07	0.10	0.27	2.02	0.99
Fe_2O_3	13.21	12.87	14.20	2.96	11.70	9.31	2.67	8.76	10.00	2.78	12.90	8.99	9.93	2.24	1.04	8.37	0.89	2.05	14.40	8.27
MnO	0.26	0.20	0.21	0.06	0.20	0.09	0.03	0.15	0.16	0.08	0.23	0.16	0.17	0.03	0.02	0.16	0.05	0.07	0.24	0.14
CaO	7.82	9.10	6.85	0.70	6.92	4.19	0.08	8.21	8.08	2.55	8.84	9.15	8.64	1.32	0.66	7.06	0.93	2.53	9.17	8.18
MgO	4.58	5.62	3.12	0.11	3.47	0.43	0.11	4.98	5.01	0.85	5.51	5.01	6.21	0.53	0.09	4.47	0.29	0.78	5.70	5.43
K_2O	1.10	0.74	1.93	4.38	1.73	1.73	5.07	1.46	1.48	3.90	0.96	1.04	1.21	4.65	5.09	2.30	5.27	3.82	0.85	1.34
Na_2O	3.32	3.09	2.96	4.85	3.63	2.98	3.87	2.98	3.06	4.53	3.13	3.33	3.26	4.57	4.10	3.25	3.20	3.14	3.12	3.04
P_2O_5	0.47	0.36	0.43	0.07	0.57	0.50	0.05	0.30	0.60	0.13	0.93	0.44	0.47	0.09	0.04	0.56	0.02	0.10	0.59	0.25
LOI	2.61	2.06	0.93	0.70	0.93	1.85	0.62	0.85	0.54	2.00	1.39	1.62	0.85	1.31	0.39	0.85	4.47	3.70	1.77	1.85
Total	99.94	100.02	100.28	99.20	99.47	100.47	98.6	99.18	98.95	99.80	100.17	100.38	100.20	99.71	98.72	100.29	100.02	99.86	100.36	99.29

Notes: Samples were analyzed by X-ray fluorescence by X-ray Assay Laboratories (XRAL) of Don Mills, Ontario, Canada. LOI—loss on ignition.

*USBM-35, USBM-75: basalt of Malheur Gorge (Evans, 1990b); AXB-715: Hunter Creek Basalt (Evans, 1990b); AXB-709: Littlefield Rhyolite (Evans, 1990b); 87-BO-35: basalt at Graveyard Point, 87-BO-29: dacite of Graveyard Point (Ferns, 1989); 87-BO-72: sanidine rhyolite intruded into ring fracture of Three Fingers caldera (Ferns, 1988); 87-BO-199, 87-BO-104: Blackjack Basalt (Ferns, 1989b); AXB-301: dam rhyodacite, AXB-308: lower Owyhee Basalt, AXB-312: upper Owyhee Basalt (Ferns and Cummings, 1992); AXB-324: basalt intrusion (Ferns and Cummings, 1992); OW-1044, OW-1481: rhyolite of Dry Creek (M.L. Cummings, 1991; unpub. data); AXB-511: basaltic andesite of Spring Mountain (MacLeod, 1990b); AWB-111: perlite from rhyolite of Double Mountain (Ramp and Ferns, 1989); AWB-100: pumice from tuff of Kern Basin (Ferns and Ramp, 1989); AWB-101: olivine basalt “Snake River type” basalt of Rock Spring (Ferns and Ramp, 1989); OW-1083: basaltic andesite of Freezeout Mountain (M.L. Cummings, 1991, unpub. data).

Idaho graben was broken by 15–20-km-wide horsts and graben into subbasins with independent histories of volcanism and sedimentation (Fig. 6, A and B).

The initial calc-alkalic volcanism during stage 2 was volumetrically the largest and formed lava flows now exposed on the north and south margins of the older intragraben calderas (Fig. 6A). More than 300 m of basalt and basaltic andesite flows (Table 2) are exposed on Spring Mountain south of Mahogany Mountain (MacLeod, 1990a, 1990b; Fig. 6A). The age of the calc-alkalic flows at Spring Mountain is fixed by their stratigraphic position between the 15.4 Ma tuff of Spring Creek and the regionally extensive 14 Ma tuff of Swisher Mountain (Fig. 6A; 14.3–13.5 Ma; Ekren et al., 1982; Armstrong et al., 1980) that entered the Oregon-Idaho graben from one or more vents located to the southeast (Ekren et al., 1982; Minor et al., 1987b; Evans et al., 1987; Evans, 1987).

Near the Owyhee dam, a rhyodacite flow-dome complex (Fig. 6A; Bryan, 1929; Table 2) attains a thickness of 330 m and buried a constructional surface developed on mafic hydrovolcanic deposits and the lower flows of the Owyhee Basalt (Fig. 6B). A K-Ar age determination for a flow in the complex is 13.5 ± 3.4 Ma (Table 1). The rhyodacite complex at the Owyhee Dam is overlain by more than 250 m of the upper Owyhee Basalt (Table 2; Bryan, 1929; Kirkham, 1931; Brown and Petros, 1985; Ferns and Cummings, 1992), a well-studied sequence of interbedded basalt to basaltic andesite flows, agglomerate, pyroclastic deposits, and volcaniclastic sediment. Brown and Petros (1985) determined that the composition of 17 of these flows is calc-alkalic; this composition was confirmed by Goles et al. (1989) and Ferns et al. (1993a).

Paleomagnetic and geochronologic studies indicate that the Owyhee Basalt erupted over a short time frame from 14.5 to 14.3 Ma based on the best K-Ar and $^{40}Ar/^{39}Ar$ age determinations. All of the age determinations range from 22.8 to 13.1 Ma (Table 1). Problems with K-Ar age determinations are illustrated by the underlying dam rhyodacite, which has yielded determinations from 22.8 ± 2.6 Ma (Brown and Petros, 1985) to 13.5 ± 3.4 Ma (Ferns and Cummings, 1992; Table 1).

In the area immediately west of Lake Owyhee (Fig. 6A), Cummings and Growney (1988) and Cummings (1991a, 1991b) described stratigraphic relations in subbasins that evolved concurrently with north-striking intragraben fault zones. Intragraben fault zones bound 10–15 km wide, roughly parallel horsts and graben. Lava-flow sequences (i.e., basalt of Hammond Hill and Blackjack Basalt in Fig. 6, A and B) establish the clearest stratigraphic correlation between neighboring subbasins and intervening horsts, but the detailed stratigraphy of basalt hydrovolcanic complexes and interfingering fluvial and lacustrine sediment define deformation across intragraben fault zones. A coherent stratigraphy has been developed in some subbasins for up to 24 km parallel to the strike of intragraben fault zones. Erosion and younger cover did not allow us to determine the segmentation of subbasins along strike of the intragraben fault zones; however, we suspect that northeast-striking faults may separate subbasins.

The intragraben fault zones served as conduits along which basalt magmas rose to the surface. Thick (>70 m) accumulations of proximal and vent facies (including intrusions) of basalt hydrovolcanic deposits mark the location of intragraben fault zones that were actively deforming during the break up of the Oregon-Idaho graben. The distal facies of these deposits are interbedded with lacustrine and fluvial, felsic-volcaniclastic sediment. Hydrovolcanic eruptions at different times and locations along the intragraben fault zones produced coalescing tuff cones and complex interfingering of sedimentary and hydrovolcanic strata.

Uplift of horst blocks is associated with a change from water-dominated, tuff-cone–forming hydroclastic eruptions to drier, cinder-cone–forming and lava-flow–producing eruptions. Some lava flows erupted within horst blocks were funneled along stream valleys into neighboring graben where the advancing flows interacted with water-saturated sediment. In addition to the lava flows, fluvial, deltaic, and lacustrine felsic-volcaniclastic sediment and basalt hydrovolcanic deposits accumulated in the neighboring graben. Similar lithologic associations and stratigraphic relations in stage 2 deposits from elsewhere in the Oregon-Idaho graben suggest that subbasins were common structural features.

The most prominent intragraben fault zones—including the Wall Rock Ridge fault zone, the Dry Creek Buttes fault zone (Cummings, 1991a, 1995; Cummings et al., 1993, 1996), and the Devils Gate fault zone (Fig. 6, A and B)—are prominent north-striking fault zones that served as magmatic and hydrothermal conduits. Each fault zone typically consists of a 2–3-km-wide zone of closely spaced, short strike-length, steeply dipping normal faults. As the fault zones exerted control on volcanism and distribution of sedimentary facies during their evolution, displacement on individual fault segments was less than 1 m, and cumulative displacement was of the order of tens of meters across a fault zone. It is possible that no surface expression of the fault

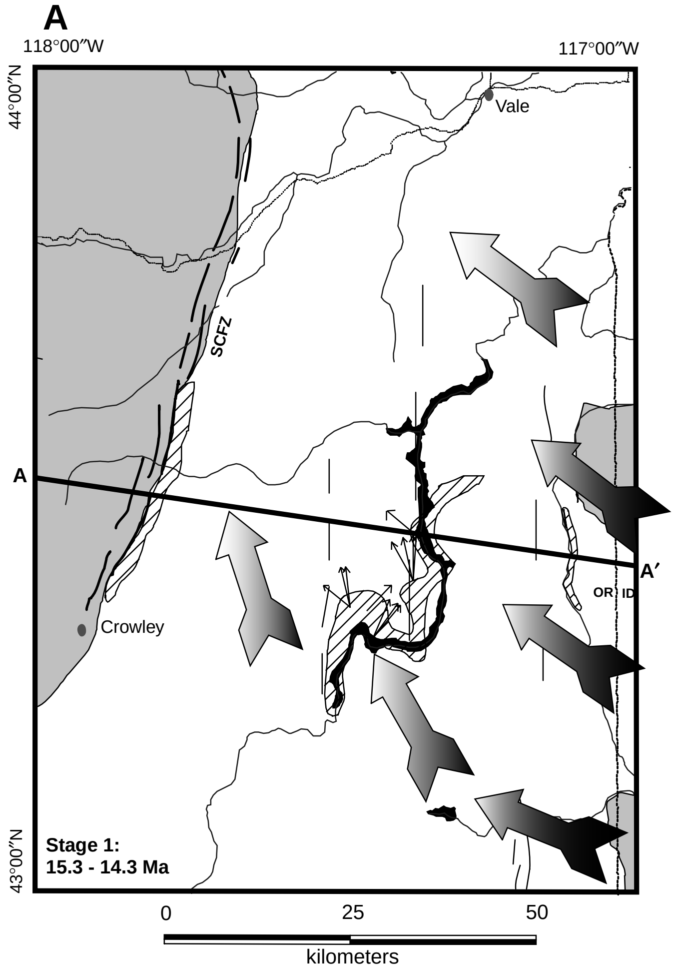

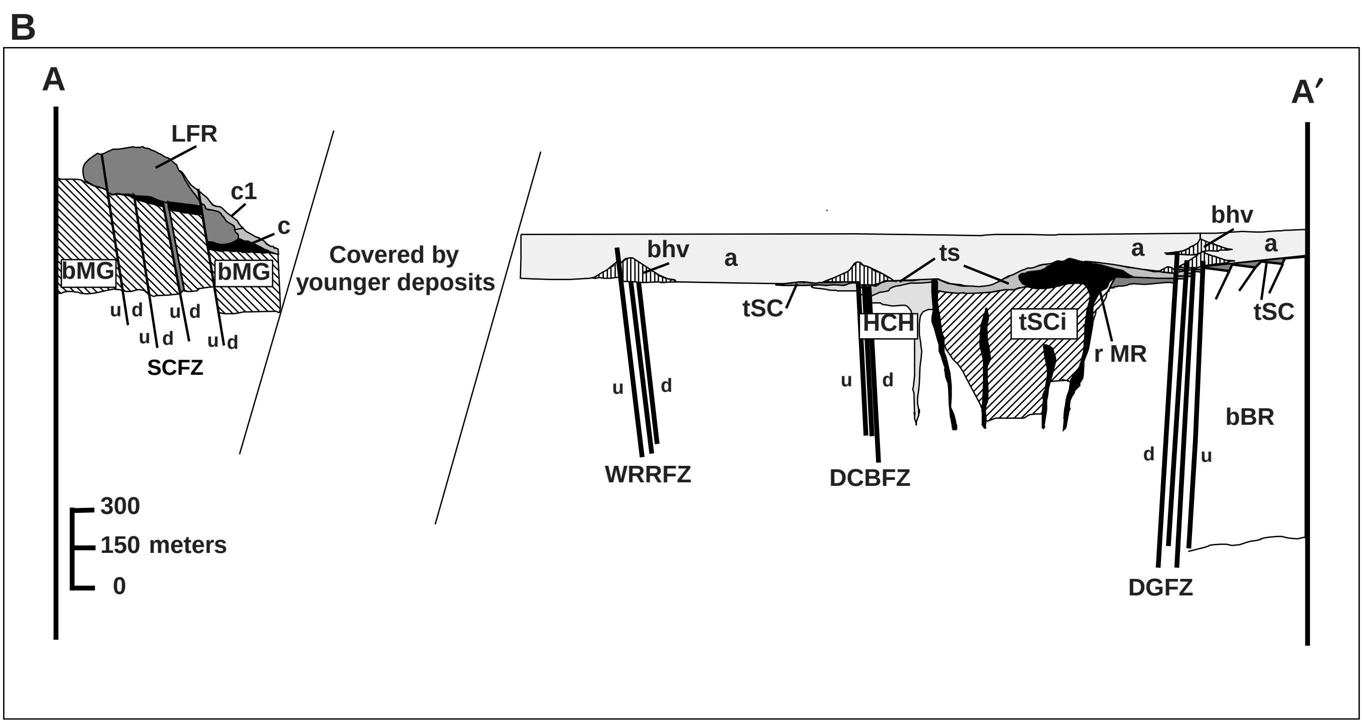

Figure 5. Stage 1. (A) Geologic features of Oregon-Idaho graben developed during stage 1 (15.3–14.3 Ma) and modern exposure of rocks of this age (ruled areas). Degree of shading in large arrows schematically illustrates decreasing arkosic component in channel sands across the graben. Paleocurrent directions are indicated by small arrows. Line weight for faults distinguishes faults of greater from lesser displacement during this time. (B) Schematic cross section along line A–A′. Symbols: a—arkosic sediments; bBR—basalt of Bishop's Ranch; bhv—basalt hydrovolcanic deposits; bMG—basalt of Malheur Gorge; c—pre–Littlefield Rhyolite conglomerate; c1—post–Littlefield Rhyolite conglomerate; DCBFZ—Dry Creek Buttes fault zone; DGFZ—Devils Gate fault zone; HCH—Honey Comb Hills; LFR—Littlefield Rhyolite; rMR—rhyolite of McIntyre Ridge; SCFZ—Squaw Creek fault zone; ts—tuffaceous sediments derived from local rhyolite flows and domes; tSC—tuff of Spring Creek; tSCi—tuff of Spring Creek intracaldera facies of Three Fingers caldera; WRRFZ—Wall Rock Ridge fault zone. ID—Idaho; OR—Oregon.

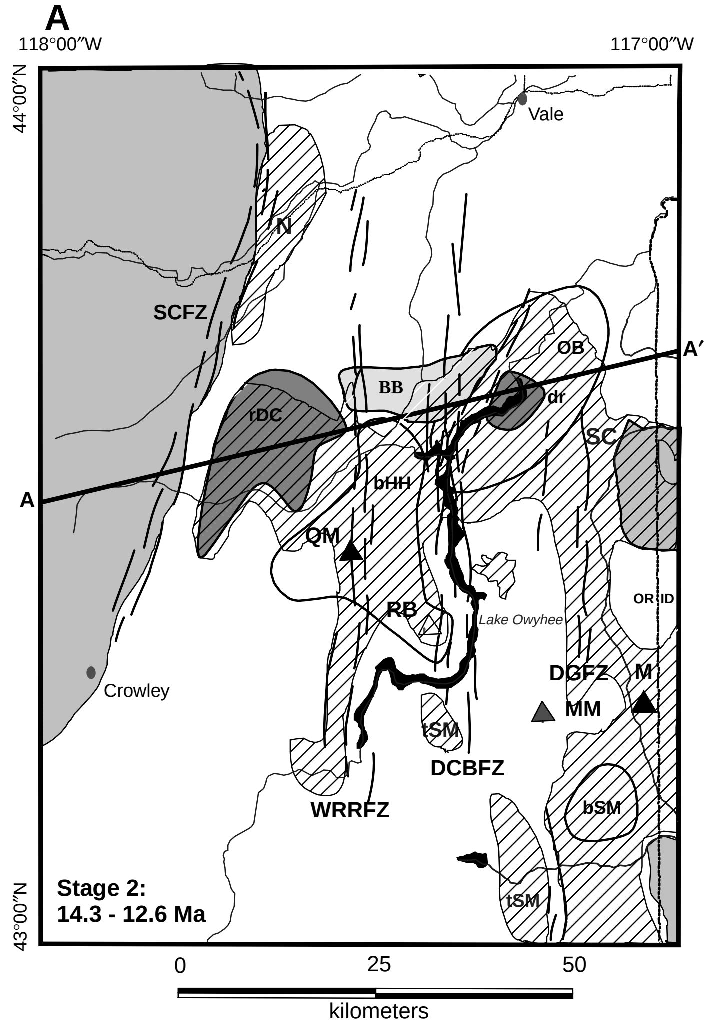

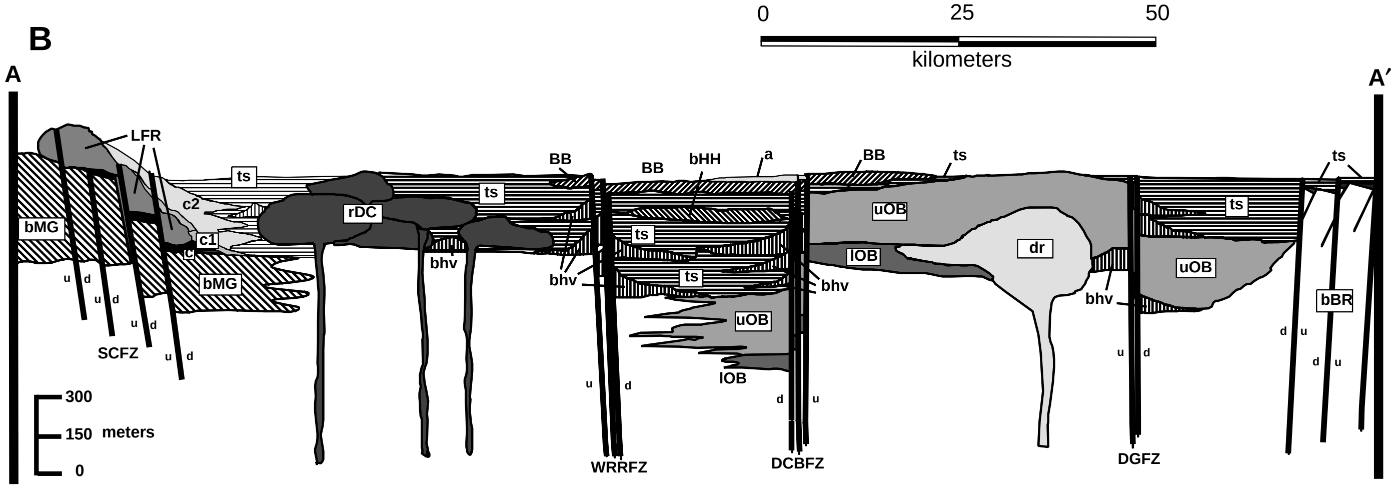

Figure 6. Stage 2. (A) Features developed in Oregon-Idaho graben during stage 2 (14.3–12.6 Ma) and modern exposure of rocks of this age (ruled pattern). (B) Schematic cross section illustrating stratigraphic relations along line A–A′. Symbols: a—arkose; BB—Blackjack Basalt; bHH—basalt of Hammond Hill; bhv—basalt hydrovolcanic deposits; bSM—basalt of Spring Mountain; bMG—basalt of Malheur Gorge; bBR—basalt of Bishop's Ranch; c—pre–Littlefield Rhyolite conglomerate; c1—conglomerate deposited during stage 1; c2—conglomerate deposited during stage 2; DCBFZ—Dry Creek Buttes fault zone; DGFZ—Devils Gate fault zone; dr—dam rhyodacite; LFR—Littlefield Rhyolite; M—Mahogany precious-metals prospect; MM—Mahogany Mountain; N—Namorf area; OB—Owyhee Basalt (lOB—lower; uOB—upper); QM—Quartz Mountain precious-metals prospect; rDC—rhyolite of Dry Creek; RB—Red Butte precious-metals prospect; SC—Succor Creek area; SCFZ—Squaw Creek fault zone; ts—tuffaceous sediment; tSM—tuff of Swisher Mountain; WRRFZ—Wall Rock Ridge fault zone. ID—Idaho; OR—Oregon.

zones occurred other than a gradual change in elevation across the zone. Over time, the greatest displacements (of more than 50 m) were localized along a few longer faults. Displacements of this magnitude produced topographic scarps that deflected drainages along the margins of subbasins. Coarse-grained detritus from partially lithified uplifted blocks was dispersed locally into the adjacent subbasins (Cummings, 1991a, 1991b). Cumulative displacements of more than 150 m typically occurred along long strike-length master faults late in the development of the intragraben fault zones. Along the Dry Creek Buttes and the Wall Rock Ridge fault zones, kink-like folds with up to 75 m between hinges evolved into north- and northeast-striking faults (Hess et al., 1996; Hess, 1998). Structural and topographic relief along portions of these intragraben fault zones may reflect reactivation during late Miocene subsidence of the western Snake River plain graben.

The Dry Creek Buttes fault zone, one of the more significant intragraben structures, marks the east flank of the area of greatest subsidence in the Oregon-Idaho graben (Fig. 6B). Maximum subsidence of at least 800 m occurred west of the zone late in stage 2 prior to eruption of the 12.8 Ma Blackjack Basalt (Kirkham, 1931; Tables 1 and 2). The Dry Creek Buttes fault zone is flanked on the east by a 15–20-km-wide horst cored by intragraben caldera rhyolite and tuff, stage 1 arkoses, and stage 2 calc-alkalic volcanics (Owyhee Basalt). In addition to basalt hydrovolcanic deposits, numerous basalt and basaltic-andesite sills and dikes were emplaced into the flanking subbasin to the west of the Dry Creek Buttes fault zone as the magmatic axis shifted westward from Owyhee Basalt vents. After eruption of the Blackjack Basalt, subsidence between the Dry Creek Buttes and Wall Rock Ridge fault zones continued and was accompanied by renewed hydrovolcanic eruptions along the Oregon-Idaho graben axis during the waning of stage 2. Subsidence of stage 2 had slowed by 12.6 Ma with the eruption of rhyolites along the Wall Rock Ridge, Dry Creek Buttes, and Devils Gate fault zones. The stratigraphy to the east and west of the Dry Creek Buttes fault zone suggests that displacement along the fault zone was down to the east as shown in Figure 5B. After eruption of the Owyhee Basalt (14.3 Ma) but prior to eruption of the Blackjack Basalt (12.8 Ma), however, the sense of displacement changed to down-to-the-west as the block containing the Owyhee Basalt and caldera-related deposits was uplifted (Fig. 6, A and B).

Muscovite-bearing arkosic fluvial sediment entered subbasins from southwestern Idaho toward the end of stage 2 and interacted with hot springs along the intragraben fault zones to produce interbedded silica-sinter deposits above large precious-metals–bearing geothermal systems (Red Butte, Quartz Mountain, Grassy Mountain, Mahogany, and Katie prospects; see Figs. 6A and 7A). Although these geothermal systems are broadly contemporaneous, each forming between 13.1 and 12.5 Ma (12.6 ± 0.6 Ma for adularia from Mahogany prospect; Table 1), and all are in part hosted by arkosic sediments, hot spring activity at each prospect passed through somewhat different stages. Mineralization at Mahogany, Red Butte, and Quartz Mountain followed stage 2 calc-alkalic mafic hydrovolcanic and lava eruptions, whereas mineralization at Katie and Grassy Mountain followed late stage 2–stage 3 silicic eruptions. Silicified fault and talus breccias and hydrothermal-eruption breccias that cut arkose-hosted sinter at Red Butte record active geysering during mineralization. Similar hydrothermal eruption breccias are present at the Katie and Mahogany prospects (Rytuba et al., 1991). At Quartz Mountain, silica-sinter clasts entrained in pre-arkose debris flows were shed off of a stage 2 hot-spring system along the Wall Rock Ridge fault zone. Later, sinter formed during arkose deposition.

Silicic magmatism marked the end of stage 2; the 12.8 Ma Bannock Ridge dome erupted along the Devils Gate fault zone, and the 12.6 Ma tuff of Kern Basin erupted from vents along the Dry Creek Buttes fault zone (Fig. 7, A and B, and Table 1).

Stage 3 (12.6–10.5 Ma)

Stage 3 is characterized by a return to basin-wide sedimentation and decreased hydrovolcanic activity and rates of magmatic output. Basaltic volcanism shifted to the west of the Wall Rock Ridge fault zone as large basaltic andesite shield volcanoes built up at Cedar Mountain and Freezeout Mountain (Table 2). The Freezeout Mountain flows, which extend north from Freezeout Mountain (Fig. 7A) for more than 40 km, yield $^{40}Ar/^{39}Ar$ age determinations between 11.5 ± 0.99 and 10.2 ± 0.94 Ma (Table 1). The Cedar Mountain flows cover approximately 800 km^2 to a depth of as much as 100 m.

The last calc-alkalic lavas erupted in the Oregon-Idaho graben were extruded from vents along the northern Dry Creek Buttes fault zone (Fig. 7A). Late stage 3 units include dacite flows north of Grassy Mountain and 8.1 Ma (Table 1) biotite-phyric rhyolites at Double Mountain (Table 2; Ramp and Ferns, 1989). High-alumina olivine tholeiite (HAOT; Hart, 1982) basalt was erupted at Grassy Mountain at 10.18 ± 1.72 Ma (Table 1).

Stage 3 sediment is mainly fluvial, extrabasinal arkose and locally derived tuffaceous lacustrine deposits. The fluvial arkoses were deposited by southeast- to northwest-flowing streams that cut across north-striking stage 2 fault zones. Although movement continued along the intragraben fault zones, they no longer controlled the distribution of sedimentary sequences. Aggrading streams carried extrabasinal granitic clasts and intrabasinal obsidian, pumice, and rhyolite clasts derived from late stage 2 and stage 3 rhyolites. Granitic clasts are more common in channel deposits, whereas volcanic clasts are more abundant in floodplain deposits. The proportion of volcanic clasts increases from east to west across the Oregon-Idaho graben. These patterns are consistent with northwest-flowing rivers with headwaters in uplifted volcanic and granitic terranes in southwestern Idaho and receiving volcanic detritus contributed by tributary streams arising in the Oregon-Idaho graben.

At this time, renewed caldera-forming rhyolitic ash-flow and large volume rhyolite lava flows erupted from vents along both flanks of the graben. The largest eruption was on the east flank where the 11.1–10.6 Ma Jump Creek Rhyolite (Fig. 7A and Table 1) covered an area of more than 100 km^2 to depths as great as 300 m (Kittleman et al., 1965, 1967). Smaller rhyolite flows and ash-flow tuffs were erupted at about 11.3 Ma (Table 1) onto the western flank at Star Mountain and Stockade Mountain (Fig. 7A). The small volume post-caldera dome at Star Mountain is highly evolved rhyolite (Table 2) associated with ferrolatites, ferroandesites, and 11.3 Ma tholeiitic basalts (Table 1).

CESSATION OF SUBSIDENCE AND INTRAGRABEN VOLCANISM

Synvolcanic subsidence along the Oregon-Idaho graben axis largely ceased by 10.5 Ma. Structural relief along the western margin was subdued by 9.68 Ma (Streck et al., 1999) when the Devine Canyon Ash-Flow Tuff (Greene et al., 1972) entered the Oregon-Idaho graben and was deposited in three cross-cutting, northwest-trending basins. Subsidence in these basins was accompanied by displacements along north- and northeast-striking faults. Major north-northeast–trending faults, such as along the west flank of Freezeout Mountain (Figs. 7B and 8; ~350 m, down to the west), offset units deposited during stage 3 and formed north-trending embayments into the Bully Creek basin (Fig. 8) which cuts across the Oregon-Idaho graben near its northern margin.

Late middle Miocene to Pliocene subsidence along the western Snake River plain was associated with the north-northeast tilt of units of the Oregon-Idaho graben by as much as 20°. Continued northward tilting of the western Snake River plain was accompanied by the development of northwest-trending fault zones across the Oregon-Idaho graben and renewed movement along the northern segments of many of the larger intragraben fault zones.

Eruption of upper Miocene (7.8 Ma, Table 1) tholeiites (Fig. 3C) within the Oregon-Idaho graben accompanied downwarping of the western Snake River plain. Subsidence along west- to northwest-trending faults across the southern part of the Oregon-Idaho graben along the Antelope Valley graben (Rytuba et al., 1991; Fig. 8) was accompanied by eruption of thin, Pliocene–Holocene tholeiitic and alkalic basalt flows (Fig. 3C and Table 1).

SYNTHESIS

The 5–6 m.y. span of synvolcanic subsidence and sedimentation in the Oregon-Idaho graben began after regional eruption of early to middle Miocene tholeiitic flood basalt and continued until the southern boundary of the West Snake River

Figure 7. Stage 3. (A) Distribution of geologic features of Oregon-Idaho graben formed during stage 3 (12.6–10.5 Ma) and approximate modern exposure of rocks of this age (ruled pattern). Shading in large arrows indicates direction of decreasing arkose content in channel sands. Paleocurrent directions are indicated by small rose diagrams. (B) Schematic cross section showing stratigraphic relations of stage 3 rock units along line A–A′. Symbols: a—arkose to tuffaceous arkose; bCM—basalt of Cedar Mountain; bFM—basalt of Freezeout Mountain; bGM—Grassy Mountain Basalt; bhv—basalt hydrovolcanic deposit; bMG—basalt of Malheur Gorge; BR—Bannock Ridge; CM—Cedar Mountain; DGFZ—Devils Gate fault zone; DCBFZ—Dry Creek Buttes fault zone; DCWT—Dinner Creek Welded Tuff; DM—Double Mountain; FM—Freezeout Mountain; GM—Grassy Mountain precious-metals prospect; HCB—Hunter Creek Basalt; JCR—Jump Creek Rhyolite; K—Katie precious-metals prospect; LFR—Littlefield Rhyolite; ri—rhyolite intrusion; SCFZ—Squaw Creek fault zone; SMC—Star Mountain caldera and Stockade Mountain; tKB—tuff of Kern Basin; tKBv—vent for tuff of Kern Basin; ts—tuffaceous sediment; WB—Westfall Butte; WRRFZ—Wall Rock Ridge fault zone. ID—Idaho; OR—Oregon.

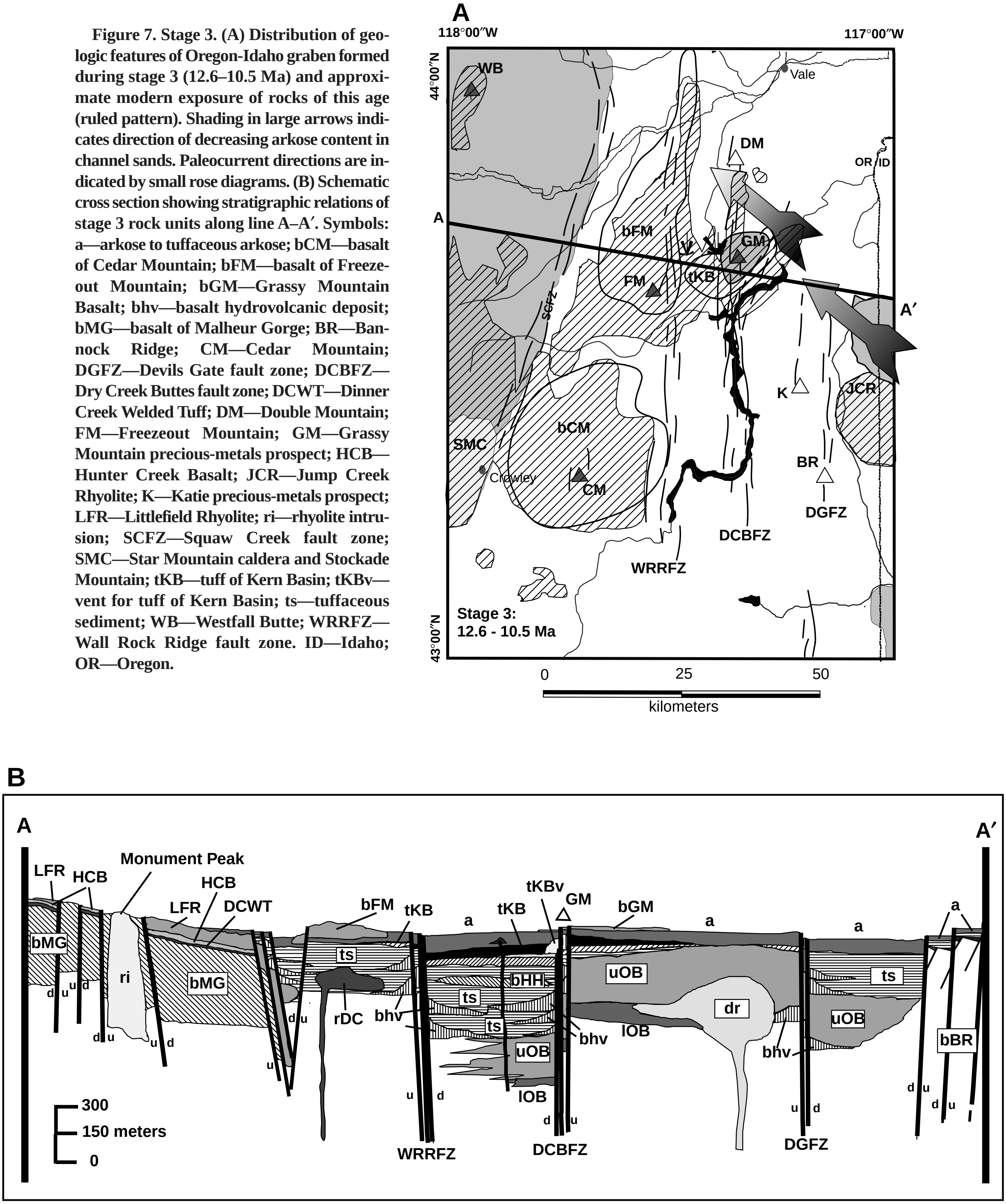

plain—defined by the Adrian fault zone—became active in the late Miocene.

Coarse-Grained Facies along Graben Margins and Intragraben Fault Zones

Coarse-grained sedimentary deposits are relatively sparse in the Oregon-Idaho graben. Tuffaceous siltstone and fine-grained, lithic-rich sandstone predominate. Coarse-grained sand to conglomerate is present in three settings: (1) along the western graben margin, (2) in fluvial channels containing extrabasinal arkosic sediment, and (3) in the vicinity of hot springs.

An abrupt change in thickness of the Littlefield Rhyolite indicates that the western margin during initial subsidence of the Oregon-Idaho graben was along the Hog Creek–Squaw Creek fault zone. The oldest conglomerates underlie the Littlefield Rhyolite (Fig. 4B, cross section B–B′) and contain angular clasts of the basalt of Malheur Gorge. As shown in Figures 5B and 6B, conglomerate was deposited during each stage of graben development. The preservation of poorly lithified sedimentary breccia clasts suggests that subsidence rates were relatively high. The youngest conglomerates contain blocks of welded tuff that are similar to 11 Ma welded tuff at Stockade Mountain and Star Mountain (Fig. 7A). Conglomerate is present up to 1.5 km east of the Squaw Creek fault zone. Relief along the western margin of the Oregon-Idaho graben persisted throughout its evolution. However, muscovite-bearing arkose deposited upon the Hunter Creek Basalt in the Little Black Canyon Quadrangle (Evans and Binger, 1998), Littlefield Rhyolite flow distribution in the Monument Peak Quadrangle (Evans, 1996), and similarities between sediment in the Tim's Peak Quadrangle (Evans and Keith, 1996) and the Oregon-Idaho graben suggest that relief along the western margin was persistent, although not present in all places at all times. Within the Oregon-Idaho graben sedimentary rocks are generally fine grained and derived from intragraben constructional highs made up of volcanic ash, rhyolite carapace breccias and vitrophyres, and mafic hydrovolcanic deposits.

Within the graben, coarse-grained deposits are most commonly conglomeratic channel facies of muscovite-bearing arkose with extrabasinal clasts of plutonic and metamorphic rocks. The greatest volume was deposited during stage 3 (Fig. 7, A and B), a time of relative tectonic quiescence within the graben. Introduction of stage 3 arkose coincided with a decrease in hydrovolcanic eruptions and increase in the eruption of mafic lava flows (Fig. 7A). Associated channel-filling lava flows and pillow-lava deltas record local areas of degradation as streams incised into the basin deposits.

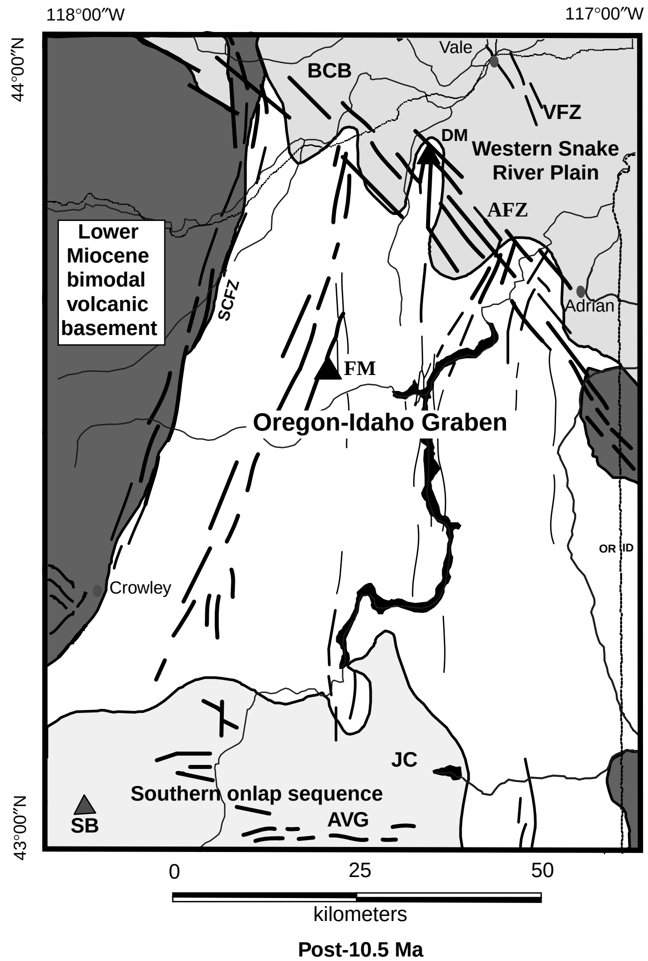

Figure 8. The Oregon-Idaho graben after approximately 10.5 Ma. Line weight for faults distinguishes faults of greater displacement from those of lesser displacement. Symbols: AFZ—Adrian fault zone; AVG—Antelope Valley graben; BCB—Bully Creek basin; DM—Double Mountain; FM—Freezeout Mountain; JC—Jordan Craters; SB—Saddle Butte; SCFZ—Squaw Creek fault zone; VFZ—Vale fault zone. ID—Idaho; OR—Oregon.

Fine-grained stage 1 and stage 2 sediments display facies changes as they thin across developing intragraben fault zones, reflecting the highly erodable nature of the poorly lithified graben-fill deposits as well as the weak topographic expression across the 2–3-km-wide fault zones. However, locally along the intragraben fault zones, the fine-grained sediment was silicified in hot springs. Clasts of hot spring sinter and silicified sediments were shed into adjoining basins where they are present in channel and beach facies (Cummings, 1991a). Sparse coarse-grained sediment was derived from coarse-grained palagonite tuff and breccia that mark vent- and proximal-facies hydrovolcanic centers that were situated along the intragraben fault zones. However, most commonly tuff cones formed local topographic highs that introduced large amounts of fine-grained palagonite into adjoining subbasins.

Volcanic Evolution Through Time

Early silicic volcanism within the Oregon-Idaho graben followed widespread tholeiitic volcanism. Initial subsidence along the Oregon-Idaho graben axis coincided with the eruption of the rhyolite of Cottonwood Mountain and the Littlefield Rhyolite lava flows from vents along the graben's west margin (Hog Creek–Squaw Creek fault zone) and caldera-forming ash flows from vents in the vicinity of the Devils Gate fault zone near the eastern margin of the graben.

A detailed discussion of the petrogenetic evolution of and dissimilarities between large rhyolite lava flows and ash-flow eruptions is beyond the scope of this paper. However, several features of the Lake Owyhee volcanic field (rhyolite flows and ash flows erupted between 15.5 and 15.0 Ma; Rytuba et al., 1991) can be noted. First, the ash-flow tuffs derived from caldera-forming eruptions differ in composition from the large rhyolite lava flows. The ash-flow tuffs range from weakly peralkaline rhyolite (comendite) to metaluminous high-silica rhyolite (Rytuba et al., 1991), whereas the large rhyolite lava flows are metaluminous, low-silica rhyolites. Second, eruptions of both were temporally and spatially associated with the waning phases of tholeiitic magmatism. The rhyolite of Cottonwood Mountain and Littlefield Rhyolite lava flows were preceded by voluminous low-alumina basalt of Malheur Gorge (Imnaha and Grande Ronde equivalent tholeiites) and locally erupted, low-alumina tholeiitic Hunter Creek Basalt. Lava flows and linear, north-striking dikes of Hunter Creek Basalt overlie and cut, respectively, the rhyolite of Cottonwood Mountain along the west edge of the Oregon-Idaho graben. The intragraben pyroclastic Leslie Gulch–Spring Creek eruptions, which followed the higher-alumina tholeiitic Bishop's Ranch eruptions, were succeeded by eruptions of small-volume, high-alumina tholeiites. Extremely iron-enriched magmatic basalt inclusions are present in caldera-fill phases of both ash flows.

Stage 2 subsidence coincided with eruption of calc-alkalic lavas (Fig. 3B) along the Oregon-Idaho graben axis and was broadly contemporaneous with similar eruptions of small-volume, extension-related, calc-alkalic lavas throughout eastern Oregon (Robyn, 1979; Bailey, 1989; Goles et al., 1989). The calc-alkalic lavas first erupted at about 14.5 Ma, approximately 0.5–1 m.y. after formation of calderas in and adjacent to the graben. Early calc-alkalic lavas erupted along a north-trending magmatic axis that was roughly coincident with the older caldera axis, suggesting that both ascended along a common north-trending structure. Exclusion of stage 2 calc-alkalic mafic lavas from the calderas may reflect a magmatic shadow caused by a cooling magma emplaced below the calderas as suggested by Rytuba and Vander Meulen (1991).

Late stage 2 and continuing into stage 3 calc-alkalic magmatism apparently occurred in pulses, switching from one intragraben fault zone to another. Initial volcanic activity along each zone was marked by hydrovolcanic eruptions from vents astride intragraben fault zones. Periods of rapid subsidence were marked by high volcanic productivity, resulting in complexly coalescing hydrovolcanic centers, thick accumulations of proximal palagonite-rich tuff, and development of thick aprons of interbedded lava flows, palagonite tuffs, and locally derived sediment. Relatively quiescent periods were marked by stream incision, introduction of extrabasinal sediment, and emplacement of intracanyon lava flows.

Syntectonic calc-alkalic volcanism within the Oregon-Idaho graben largely ceased following eruption of large-volume rhyolite lava flows and caldera-related ash-flow tuffs from vents along both flanks starting at about 11 Ma. Physical characteristics of the flanking rhyolites, including a rheomorphic ash-flow tuff at Stockade Mountain on the west flank and the large-volume Jump Creek rhyolite lava flow on the east flank are indicative of high eruption temperatures. The switch from intragraben calc-alkalic volcanism to extragraben high-temperature rhyolite volcanism marked the start of large-volume caldera-forming rhyolite eruptions along an age pattern that becomes younger westward across central Oregon (MacLeod et al., 1976; Walker and MacLeod, 1991).

Geothermal Evolution

Large geothermal cells developed along the intragraben fault zones during stage 2 and stage 3 subsidence, forming hot-spring and epithermal prospects (Au, Ag, and Hg). Bedded sinter, hydrothermal eruption breccias, and exhalative chert mark where hot springs vented at the paleosurface. Large, better-known systems, such as Grassy Mountain (Fig. 7, A and B), Quartz Mountain, Red Butte, Mahogany (Fig. 6A), and Katie (Fig. 7A) (Evans, 1986; Gilbert, 1988; Rytuba et al., 1991; Zimmerman, 1991; Zimmerman and Larson, 1994; Cummings, 1991a, 1995) are all hosted in late stage 2 or stage 3 arkose or volcaniclastic sediments and are associated spatially with either basalt or rhyolite vents.

The peak period of mineralization closely followed rapid synvolcanic subsidence near the end of stage 2 as meteoric water intermixed along the same intragraben fault zones that served as magmatic conduits. Hot springs interacted with fluvial sediment deposited as streams flowed into the Oregon-Idaho graben from the east.

Spatial and temporal relationships between intragraben fault zones, hydrovolcanic vents, and geothermal cells indicate that middle Miocene hydrothermal activity peaked during a time of decreasing synvolcanic subsidence along intragraben fault zones. The coincidental incursion of fluvial arkoses into the Oregon-Idaho graben at this time corresponded with decreased hydrovolcanic activity and intragraben subsidence. It thus appears that mineralization is more closely linked to cycles of syntectonic calc-alkalic volcanism than to caldera foundering following emplacement of batholith-sized subcaldera intrusions as suggested by Rytuba and Vander Meulen (1991) and Rytuba (1994). Cummings et al. (1996) suggested hot spring activity at two large prospects—Red Butte and Quartz Mountain—followed emplacement of a thick gabbro intrusion in the graben axial zone.

CONCLUSIONS

The Oregon-Idaho graben evolved as part of a north- to northwest-trending, 1100-km-long middle Miocene synvolcanic rift system that included the northern Nevada rift, Baker graben, and Columbia River Basalt dike swarms. The northerly trend of the Oregon-Idaho graben may be a structural expression of the Mesozoic craton margin. Extension along the least-principal-stress direction, as indicated by orientation of syntectonic dikes, was consistently oriented east-west during graben subsidence. Initial graben subsidence at approximately 15.4 Ma was accompanied by eruptions of large-volume rhyolite lava flows and caldera-forming ash-flow tuffs.

The graben evolved through three stages: (1) incursion of fluvial arkoses across a basin the topographic highs of which were constructional volcanic features associated with caldera-related resurgent domes and coalescing silicic tuff cones (15.4–14.3 Ma); (2) breakup of the graben floor into intragraben subbasins during eruption of calc-alkalic magmas (14.3–12.6 Ma); and (3) return to aggrading, basin-wide sedimentation accompanied by reduced rates of subsidence and waning volcanic and geothermal activity (12.6–10.5 Ma). During stage 2, topographic highs were mainly constructional features formed by mafic volcanic and hydrovolcanic vents located along north-trending intragraben fault zones. Reduced rates of magmatism during stage 2 coincided with local erosion along fault scarps, late incursion of arkose-laden fluvial systems, and initiation of large precious-metals-bearing geothermal systems.

The Oregon-Idaho graben ceased to be an important synvolcanic graben about 11 Ma, during the switch from intragraben calc-alkalic volcanism to region-wide eruption of high-alumina olivine basalt (Carlson and Hart, 1987) and extragraben high-temperature rhyolite volcanism that marked the initiation of the westward-younging rhyolite pattern across central Oregon (MacLeod et al., 1976; Walker and MacLeod, 1991). Late Miocene and younger subsidence, volcanism, and hydrothermal activity were related to reoriented regional stresses associated with the northwest-trending western Snake River plain and the east-west–trending Antelope Valley graben.

ACKNOWLEDGMENTS

Geologic mapping was supported by the Oregon State Lottery Fund for Economic Development and U.S. Geological Survey (COGEOMAP).

Portland State University participation was funded in part by National Science Foundation Research Experiences for Undergraduates grant EAR-9200217, and by private mining interests, the Geological Society of the Oregon Country, and student tuition and fees. Early reviews by Spencer Wood and Gary Smith provided helpful suggestions for improvement. Technical reviews by James Rytuba, Richard Conrey, and Gary Smith helped us refine this paper for publication.

REFERENCES CITED

Alt, D., Sears, J.W., and Hyndman, D., 1988, Terrestrial maria, the origins of large basalt plateaus, hotspot tracks, and spreading ridges: Journal of Geology, v. 96, p. 647–662.

Armstrong, R.L., Taubeneck, W.H., and Hales, P.O., 1977, Rb-Sr and K-Ar geochronometry of Mesozoic granitic rocks and their Sr isotopic composition, Oregon, Washington, and Idaho: Geological Society of America Bulletin, v. 88, p. 397–411.

Armstrong, R.L., Harakal, J.E., and Neill, W.M., 1980, K-Ar dating of Snake River Plain (Idaho) volcanic rocks—New results: Isochron/West, no. 27, p. 5–10.

Bailey, D.G., 1989, Calc-alkalic volcanism associated with crustal extension in northeastern Oregon: New Mexico Bureau of Mines and Mineral Resources Bulletin 131, p. 12.

Baksi, A.K., 1989, Reevaluation of the timing and duration of extrusion of the Imnaha, Picture Gorge, and Grande Ronde Basalts, Columbia River Basalt Group, *in* Reidel, S.P., and Hooper, P.R., eds., Volcanism and tectonism in the Columbia River flood-basalt province: Geological Society of America Special Paper 239, p. 105–111.

Benson, G.T., and Kittleman, L.R., 1968, Geometry of flow layering in silicic lavas: American Journal of Science, v. 266, p. 265–276.

Binger, G.B., 1997, The volcanic stratigraphy of the Juntura region, eastern Oregon: Pullman, Washington [Master's thesis]: Pullman, Washington State University, 206 p.

Blank, H.R., Jr., and Gettings, M.E., 1974, Geophysical evidence of caldera structures in the Harney Basin of central eastern Oregon [abs.]: Eos (Transactions, American Geophysical Union), v. 55, no. 5, p. 557.

Bottomley, R.J., and York, D., 1976, $^{40}Ar/^{39}Ar$ age determinations on the Owyhee Basalt of the Columbia Plateau: Earth and Planetary Science Letters, v. 31, p. 75–84.

Brandon, A.D., and Goles, G.G., 1988, A Miocene subcontinental plume in the Pacific Northwest: Geochemical evidence: Earth and Planetary Science Letters, v. 88, p. 273–283.

Brooks, H.C., Ferns, M.L., Nusbaum, R.W., and Kovich, P.M., 1979, Geologic map of the Rastus Mountain Quadrangle, Oregon: Oregon Department of Geology and Mineral Industries Open-File Report O-79-07, scale 1:24 000.

Brooks, H.C., and O'Brien, J.P., 1992, Geology and mineral resource map of the Westfall Quadrangle, Malheur County, Oregon: Oregon Department of Geology and Mineral Industries Geological Map Series GMS-71, 1:24 000.

Brown, D.E., and Petros, J.R., 1985, Geochemistry, geochronology, and magnetostratigraphy of a measured section of the Owyhee Basalt, Malheur County, Oregon: Oregon Geology, v. 47, p. 15–20.

Bryan, K., 1929, Geology of reservoir and dam sites, with a report on the Owyhee Irrigation Project, Oregon: U.S. Geological Survey Water-Supply Paper 597-A, 72 p.

Carlson, R.W., and Hart, W.K., 1987, Crustal genesis on the Oregon Plateau: Journal of Geophysical Research, v. 92, p. 6191–6206.

Carlson, R.W., and Hart, W.K., 1988, Flood basalt volcanism in the northwestern United States, *in* MacDougall, J.D., ed., Continental flood basalts: Boston, Kluwer Academic Publishers, p. 35–61.

Carmichael, I.S.E., 1964, The petrology of Thingmuli, a Tertiary volcano in eastern Iceland: Journal of Petrology, v. 5, p. 435–460.

Cummings, M.L., 1991a, Geology of the Deer Butte Formation, Malheur County, Oregon: Faulting, sedimentation, and volcanism in a post-caldera setting, *in* Cas, R., and Busby-Spera, C., eds., Volcaniclastic sedimentation: Sedimentary Geology, v. 74, p. 345–362.

Cummings, M.L., 1991b, Relations among volcaniclastic sedimentation, volcanism, faulting, and hydrothermal activity west of Lake Owyhee, Malheur County, Oregon, *in* Raines, G., Lisle, R.E., Schafer, R.W., and Wilkinson, W.H., eds., Geology and ore deposits of the Great Basin: Geological Society of Nevada, Symposium Proceedings, v. 1, p. 111–132.

Cummings, M.L., 1995, Intragraben fault zones, volcanism, and geothermal evolution in the Oregon-Idaho graben, U.S.A.: PACRIM Congress 1995, Australasian Institute of Mining and Metallurgy Publication Series No. 9/95, p. 169–174.

Cummings, M.L., and Growney, L.P., 1988, Basalt hydrovolcanic deposits in the Dry Creek Arm area of the Owyhee Reservoir, Malheur County, Oregon: Stratigraphic relations: Oregon Geology, v. 50, no. 7/8, p. 75–82, 94.

Cummings, M.L., Ebeling, C., and Johnson, A.G., 1993, North-striking fault zones and evolution of the central graben, Ore-Ida graben Malheur County, Oregon: Geological Society of America Abstracts with Programs, v. 25, no. 6, p. 26.

Cummings, M.L., Evans, J.G., and Ferns, M.L., 1994, Stratigraphic and structural evolution of the middle Miocene Oregon-Idaho graben Malheur County, Oregon, *in* Swanson, D.A., and Haugerud, R.S., eds., Geologic field trips in the Pacific Northwest, 1994 Geological Society of America Annual Meeting, Seattle, Washington, v. 1, page lG-1–lG-20.

Cummings, M.L., Johnson, A.G., and Cruikshank, K.M., 1996, Intragraben fault zones and hot-spring deposits in the Oregon-Idaho graben: A geophysical study, *in* Coyner, A.R., and Fahey, P.L., eds., Geology and ore deposits of the American Cordillera: Geological Society of Nevada Symposium, Reno/Sparks, Nevada, April 1995, p. 1047–1062.

Draper, D.S., 1991, Late Cenozoic bimodal magmatism in the northern Basin and Range province of southeastern Oregon: Journal of Volcanology and Geothermal Research, v. 47, p. 299–328.

Duffield, W.A., and McKee, E.H., 1986, Geochronology, structure, and basin-range tectonism of the Warner Range, northeastern California: Geological Society of America Bulletin, v. 97, p. 142–146.

Eaton, G.P., 1984, The Miocene Great Basin of western North America as an extended back-arc region: Tectonophysics, v. 102, p. 275–295.

Ekren, E.B., McIntyre, D.H., Bennett, E.H., and Malde, H.E., 1981, Geologic map of Owyhee County, Idaho, west of longitude 116°W: U.S. Geological Survey Miscellaneous Investigations Series Map I-1256, scale 1:125 000.

Ekren, E.B., McIntyre, D.H., Bennett, E.H., and Marvin, R.F., 1982, Cenozoic stratigraphy of western Owyhee County, Idaho, *in* Bonnichsen, B., and Breckenridge, R.M., eds., Cenozoic geology of Idaho: Idaho Geological Survey Bulletin 26, p. 215–235.

Evans, C.S., 1986, The geology, geochemistry, and alteration of Red Butte, Oregon: A precious metal-bearing paleohot spring system [Master's thesis]: Portland, Oregon, Portland State University, 133 p.

Evans, J.G., 1987, Geologic map of the Owyhee Canyon Wilderness study area, Malheur County, Oregon: U.S. Geological Survey Miscellaneous Field Studies Map MF-1926, scale 1:62 500.

Evans, J.G., 1990a, Geology and mineral resources map of the Jonesboro Quadrangle, Malheur County, Oregon: Oregon Department of Geology and Mineral Industries Geological Map Series GMS-66, scale 1:24 000.

Evans, J.G., 1990b, Geology and mineral resources map of the South Mountain Quadrangle, Malheur County, Oregon: Oregon Department of Geology and Mineral Industries Geological Map Series GMS-67, scale 1:24 000.

Evans, J.G., 1992, Geologic map of the Dooley Mountain Quadrangle, Baker County, Oregon: U.S. Geological Survey GQ-1694, scale 1:24 000.

Evans, J.G., 1996, Geologic map of the Monument Peak Quadrangle, Malheur County, Oregon: U.S. Geological survey Miscellaneous Field Studies Map MF-2317, scale 1:24 000.

Evans, J.G., and Binger, G.B., 1997, Geologic map of the Westfall Butte Quadrangle, Malheur County, Oregon: U.S. Geological Survey Open-File Report 97-481, scale 1:24 000.

Evans, J.G., and Binger, G.B., 1998, Geologic map of Little Black Canyon Quadrangle, Malheur County, Oregon: U.S. Geological Survey Open-File Report 98-493, scale 1:24 000.

Evans, J.G., and Keith, W.J., 1996, Geologic map of the Tims Peak Quadrangle, Malheur County, Oregon: U.S. Geological Survey Miscellaneous Field Studies Map MF-2316, scale 1:24 000.

Evans, J.G., Hoffman, J.D., Kulik, D.M., and Linne, J.M., 1987, Mineral resources of the Owyhee Canyon Wilderness study area, Malheur County, Oregon: U.S. Geological Survey Bulletin 1719-E, 18 p.

Ferns, M.L., 1988, Geology and mineral resources map of the Owyhee Ridge Quadrangle, Malheur County, Oregon: Oregon Department of Geology and Mineral Industries Geological Map Series GMS-53, scale 1:24 000.

Ferns, M.L., 1989, Geology and mineral resources map of the Graveyard Point Quadrangle, Malheur County, Oregon, and Owyhee County, Idaho: Oregon Department of Geology and Mineral Industries Geological Map Series GMS-54, scale 1:24 000.

Ferns, M.L., and Cummings, M.L., 1992, Geology and mineral resources map of The Elbow Quadrangle, Malheur County, Oregon: Oregon Department of Geology and Mineral Industries Geological Map Series GMS-74, scale 1:24 000.

Ferns, M.L., and Williams, C., 1993, Preliminary geologic map of the Crowley Quadrangle, Malheur County, Oregon: Oregon Department of Geology and Mineral Industries Open-file Report O-93-4, scale 1:24 000.

Ferns, M.L., Brooks, H.C., Evans, J.G., and Cummings, M.L., 1993a, Geologic map of the Vale 30 × 60 minute quadrangle, Malheur County, Oregon, and Owyhee County, Idaho: Oregon Department of Geology and Mineral Industries Geological Map Series GMS-77, scale 1:100 000.

Ferns, M.L., Evans, J.G., and Cummings, M.L., 1993b, Geologic map of the Mahogany Mountain 30 × 60 minute quadrangle, Malheur County, Oregon, and Owyhee County, Idaho: Oregon Department of Geology and Mineral Industries Geologic Map Series GMS-78, scale 1:100 000.

Fiebelkorn, R.B., Walker, G.W., MacLeod, N.S., McKee, E.H., and Smith, J.G., 1983, Index to K-Ar age determinations for the State of Oregon: Isochron/West, no. 37, p. 3–60.

Geist, D., and Richards, M., 1993, Origin of the Columbia Plateau and Snake River plain: Deflection of the Yellowstone plume: Geology, v. 21, p. 789–792.

Gilbert, D., 1988, Geology and geochemistry of the Mahogany hot-springs gold prospect in the Owyhee region of southeastern Oregon [Master's thesis]: Seattle, University of Washington, 76 p.

Goles, G.G., Brandon, A.D., and Lambert, R.StJ., 1989, Miocene basalts of the Blue Mountain province in Oregon; Part 2, Sr isotopic ratios and trace element features of little-known Miocene basalts of central and eastern Oregon, in Reidel, S.P., and Hooper, P.R., eds., Volcanism and tectonism in the Columbia River flood-basalt province: Geological Society of America Special Paper 239, p. 357–365.

Greene, R.C., Walker, G.W., and Corcoran, R.E., 1972, Geologic map of the Burns Quadrangle, Oregon: U.S. Geological Survey Miscellaneous Investigations Map I-680, scale 1:250 000.

Haddock, G.H., 1967, The Dinner Creek Welded Ash-Flow Tuff of the Malheur Gorge area, Malheur County, Oregon [Ph.D. dissert.]: Eugene, University of Oregon, 111 p.

Hart, W.K., 1982, Chemical, geochronologic and isotopic significance of low K, high-alumina olivine tholeiite in the northwestern Great Basin, U.S.A. [Ph.D. dissert.]: Cleveland, Ohio, Case Western Reserve University, 410 p.

Hart, W.K., and Mertzman, S.A., 1983, Late Cenozoic volcanic stratigraphy of the Jordan Valley area, southeastern Oregon: Oregon Geology, v. 45, no. 2, p. 15–19.

Hart, W.K., Aronson, J.L., and Mertzman, S.A., 1984, Areal distribution and age of low-K, high alumina olivine tholeiite magmatism in the northwestern Great Basin: Geological Society of America Bulletin, v. 95, p. 185–195.

Hart, W.K., Carlson, R.W., and Mosher, S.A., 1989, Petrogenesis of the Pueblo Mountains basalt, southeastern Oregon and northwestern Nevada, *in* Reidel, S.P., and Hooper, P.R., eds., Volcanism and tectonism in the Columbia River flood-basalt province: Geological Society of America Special Paper 239, p. 367–378.

Hess, S.R., 1998, Structural evolution of the Dry Creek Buttes fault zone, Malheur County, Oregon [M.S. thesis]: Portland, Oregon, Portland State University, 130 p.

Hess, S.R., Cruikshank, K.M., and Cummings, M.L., 1996, Structural evolution of the Burnt Mountain strand, Dry Creek Buttes fault zone, Oregon-Idaho graben, eastern Oregon: Geological Society of America Abstracts with Programs, v. 28, no. 5, p. 75.

Hooper, P.R., and Conrey, R.M., 1989, A model for the tectonic setting of the Columbia River basalt eruptions, *in* Reidel, S.P., and Hooper, P.R., eds., Volcanism and tectonism in the Columbia River flood-basalt province: Geological Society of America Special Paper 239, p. 293–306.

Kirkham, V.R.D., 1931, Revision of the Payette and Idaho formations: Journal of Geology, v. 39, p. 193–239.

Kittleman, L.R., Green, A.R., Hagood, A.R., Johnson, A.M., McMurray, J.M., Russell, R.G., and Weeden, D.A., 1965, Cenozoic stratigraphy of the Owyhee region, southeastern Oregon: Eugene, University of Oregon Museum of Natural History Bulletin 1, 45 p.

Kittleman, L.R., Green, A.R., Haddock, G.H., Hagood, A.R., Johnson, A.M., McMurray, J.M., Russell, R.G., and Weeden, D.A., 1967, Geologic map of the Owyhee region, Malheur County, Oregon: Eugene, University of Oregon Museum of Natural History Bulletin 8, scale 1:125 000.

Lawrence, D.C., 1988, Geologic field trip guide to the northern Succor Creek area, Malheur County, Oregon: Oregon Geology, v. 50, p. 15–21.

Leeman, W.P., Oldow, J.S., and Hart, W.K., 1992, Lithosphere-scale thrusting in the western U.S. Cordillera as constrained by Sr and Nd isotopic transitions in Neogene volcanic rocks: Geology, v. 20, p. 63–66.

Lees, K.R., 1994, Magmatic and tectonic changes through time in the Neogene volcanic rocks of the Vale area, Oregon, northwestern USA [Ph.D. dissert.]: Milton Keynes, UK, Open University, 284 p.

MacLeod, N.S., 1990a, Geology and mineral resources map of the Mahogany Gap Quadrangle, Malheur County, Oregon: Oregon Department of Geology and Mineral Industries Geological Map Series GMS-65, scale 1:24 000.

MacLeod, N.S., 1990b, Geology and mineral resources map of the Sheaville Quadrangle, Malheur County, Oregon, and Owyhee County, Idaho: Oregon Department of Geology and Mineral Industries Geological Map Series GMS-64, scale, 1:24 000.

MacLeod, N.S., Walker, G.W., and McKee, E.H., 1976, Geothermal significance of eastward increase in age of upper Cenozoic rhyolite domes in southeastern Oregon: Proceeding Second United Nations Symposium on Development and Use of Geothermal Resources, v. 1, p. 465–474.

Magill, J., and Cox, A., 1981, Post-Oligocene tectonic rotation of the Oregon western Cascade Range and the Klamath Mountains: Geology, v. 9, p. 127–131.

Mathis, A.C., 1993, Geology and petrology of a 26-Ma trachybasalt to peralkaline rhyolite suite exposed at Hart Mountain, southern Oregon [Master's thesis]: Corvallis, Oregon State University, 141 p.

Minor, S.A., Plouff, D., Esparza, L.E., and Peters, T.J., 1987a, Mineral resources of the High Steens and Little Blitzen Gorge Wilderness study areas, Harney County, Oregon: U.S. Geological Survey Bulletin 1740-A, 21 p.

Minor, S.A., King, H.D., Kulik, D.M., and Sawatzky, D.L., 1987b, Mineral resources of the upper Deep Creek Wilderness study area, Owyhee County, Idaho: U.S. Geological Survey Bulletin 1719-G, 14 p.

Myashiro, A., 1975, Volcanic rock series and tectonic setting: Annual Review of Earth and Planetary Sciences, v. 3, p. 251–269.

Pansze, A.J., Jr., 1975, Geology and ore-deposits of the Silver City–DeLamar–Flint region, Owyhee County, Idaho: Idaho Bureau of Mines and Geology Pamphlet 161, 79 p.

Pierce, K.L., and Morgan, L.A., 1992, The track of the Yellowstone hot spot: Volcanism, faulting, and uplift, *in* Link, P.K., Kuntz, M.A., and Platt, L.B., eds., Regional geology of eastern Idaho and western Wyoming: Geological Society of America Memoir 179, p. 1–53.

Plumley, P.S., 1986, Volcanic stratigraphy and geochemistry of the Hole in the Ground area, Owyhee Plateau, southeastern Oregon [Master's thesis]: Moscow, University of Idaho, 161 p.

Ramp, L., and Ferns, M.L., 1989, Geology and mineral resources map of the Double Mountain Quadrangle, Malheur County, Oregon: Oregon Department of Geology and Mineral Industries Geological Map Series GMS-58, scale 1:24 000.

Robyn, T.L., 1979, Miocene volcanism in eastern Oregon: An example of calc-alkalic volcanism unrelated to subduction: Journal of Volcanology and Geothermal Research, v. 5, p. 149–161.

Rytuba, J.J., 1994, Evolution of volcanic and tectonic features in caldera settings and their importance in the localization of ore deposits: Economic Geology, v. 89, p. 1687–1696.

Rytuba, J.J., and McKee, E.H., 1984, Peralkaline ash flow tuffs and calderas of the McDermitt volcanic field, southeast Oregon and north central Nevada: Journal of Geophysical Research, v. 89, p. 8616–8628.

Rytuba, J.J., Vander Meulen, D.B., and Minor, S.A., 1989, Geologic evolution of the Three Fingers caldera, Malheur County, Oregon: Geological Society of America Abstracts with Programs, v. 21, no. 5, p. 138.

Rytuba, J.J., Vander Meulen, D.B., and Barlock, V.E., 1991, Tectonic and stratigraphic controls on epithermal precious metal mineralization in the northern part of the Basin and Range, Oregon, Idaho, and Nevada, *in* Buffa, R.H., and Coyner, A.R., eds., Geology and ore deposits of the Great Basin field trip guidebook compendium: Geological Society of Nevada, v. 2, p. 633–644.

Rytuba, J.J., and Vander Meulen, D.B., 1991, Hot-spring precious-metal systems in the Lake Owyhee volcanic field, Oregon-Idaho, *in* Raines, G., Lisle, R.E., Schafer, R.W., and Wilkinson, W.H., eds., Geology and ore deposits of the Great Basin: Geological Society of Nevada Symposium Proceedings, v. 2, p. 1085–1096.

Streck, M.J., Johnson, J.A., Grunder, A.L., 1999, Field guide to the Rattlesnake Tuff and High Lava Plains near Burns, Oregon: Oregon Geology, v. 61, no. 3, p. 64–76.

Tolan, T.L., Reidel, S.P., Beeson, M.H., Anderson, J.L., Fecht, K.R., and Swanson, D.A., 1989, Revisions to the estimates of the areal extent and volume of the Columbia River Basalt Group, *in* Reidel, S.P., and Hooper, P.R., eds., Volcanism and tectonism in the Columbia River flood-basalt province: Geological Society of America Special Paper 239, p. 1–20.

Vander Meulen, D.B., 1989, Intracaldera tuffs and central-vent intrusion of the Mahogany Mountain caldera, eastern Oregon: U.S. Geological Survey Open-File Report 89-77, 69 p., 2 plates, map scale 1:72 750.

Vander Meulen, D.B., Rytuba, J.J., Vercoutere, T.L., and Minor, S.A., 1987, Geologic map of the Rooster Comb 7.5′ quadrangle, Malheur County, Oregon: U.S. Geological Survey Miscellaneous Field Studies Map, MF-1902C, scale 1:24 000.

Vander Meulen, D.B., Griscom, A., King, H.D., and Moyle, P.R., 1988, Mineral resources of the Blitzen River Wilderness study area, Harney County, Oregon: U.S. Geological Survey Bulletin 1740-D, 14 p.

Walker, G.W., 1990, Miocene and younger rocks of the Blue Mountains region, exclusive of the Columbia River Basalt Group and associated mafic lava flows, *in* Walker, G.W., ed., Geology of the Blue Mountains region of Oregon, Idaho, and Washington: Cenozoic geology of the Blue Mountains region: U.S. Geological Survey Professional Paper 1437, p. 101–118.

Walker, G.W., and MacLeod, N.S., 1991, Geologic map of Oregon: U.S. Geological Survey special map, scale 1:500 000.

Wallace, A.B., Noble, C.D., and Grant, N.K., 1980, Icelandite- and aenigmatite-bearing pantellerite from the McDermitt caldera complex, Nevada-Oregon: Geology, v. 8, p. 380–384.

Watkins, N.D., and Baksi, A.K., 1974, Magnetostratigraphy and oroclinal folding of the Columbia River, Steens, and Owyhee basalts in Oregon, Washington, and Idaho: American Journal of Science, v. 274, p. 148–189.

Wells, R.E., 1979, Drake Peak—A structural complex rhyolite center in southeastern Oregon: U.S. Geological Survey Professional Paper 1124-E, p. E1–E16.

Zimmerman, B.S., 1991, Geology and geochemistry of epithermal gold mineralization in the Lake Owyhee volcanic field—Western Snake River plain region of eastern Oregon and western Idaho [Ph.D. dissert.]: Pullman, Washington State University, 262 p.

Zimmerman, B.S., and Larson, P.B., 1994, Epithermal gold mineralization in a fossil hot spring system, Red Butte, Oregon: Economic Geology, v. 89, p. 1983–2002.

Zoback, M.L., and Thompson, G.A., 1978, Basin and Range rifting in northern Nevada: Clues from a mid-Miocene rift and its subsequent offsets: Geology, v. 6, p. 111–116.

Zoback, M.L., McKee, E.H., Blakely, R.J., and Thompson, G.A., 1994, The northern Nevada rift: Regional tectono-magmatic relations and middle Miocene stress directions: Geological Society of America Bulletin, v. 106, p. 371–382.

MANUSCRIPT RECEIVED BY THE SOCIETY JUNE 23, 1997
REVISED MANUSCRIPT RECEIVED MAY 4, 1999
MANUSCRIPT ACCEPTED MAY 11, 1999

Printed in USA